National Synchrotron Light Source II (NSLS-II): Present status and upgrade plans

Guimei Wang
NSLS-II, Brookhaven National Lab
Oct. 30th, 2020
MSU-FRIB Accelerator Physics and Engineering Webinar

U.S. DEPARTMENT OF ENERGY | Office of Science

BROOKHAVEN NATIONAL LABORATORY

Outline

Present status

- Overview
- Machine key performance
  - Beam emittance
  - Beam stability
  - Operation reliability
  - High current

Upgrade plans

- Trend in synchrotron light sources: today → tomorrow
- Complex bend
  - Properties of the element
  - Integration into lattice design
  - Magnet design
  - Prototype of Complex Bend
- Summary and outlook

Overview

National Synchrotron Light Source II

- NSLS-II is a 3 GeV, 500 mA, high-brightness light source, funded by U.S. Department of Energy (DOE), at the Brookhaven National Laboratory
- One of the newest and most advanced synchrotron facilities in the world.
  - wide spectral range: IR to hard x-ray
  - high average spectral brightness
  - high flux density
  - >60 beamlines

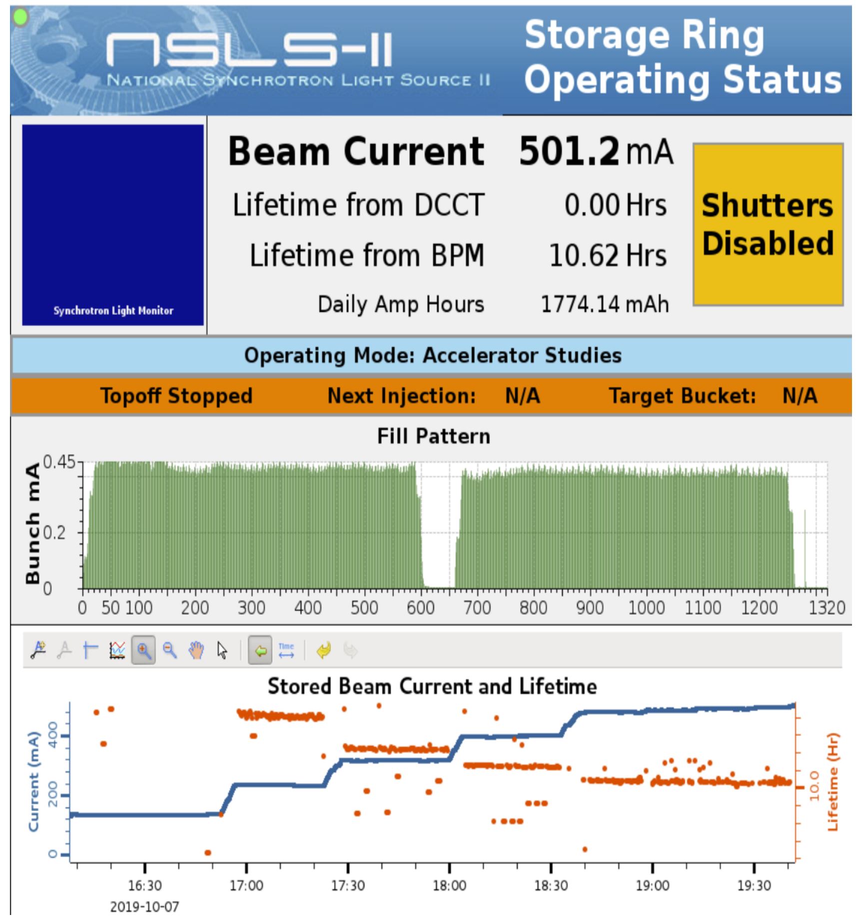

- CD-0 was approved in 2005
- CD-3 was approved in 2009
- SR commissioning started in Mar. 2014
- In Feb. 2015, CD-4, the final milestone of the project, completed
- Total cost is $912 Million
- 28 beamlines in top off operation at 400 mA
- Oct. 2019, demonstrated 500 mA beam current

Brookhaven National Laboratory

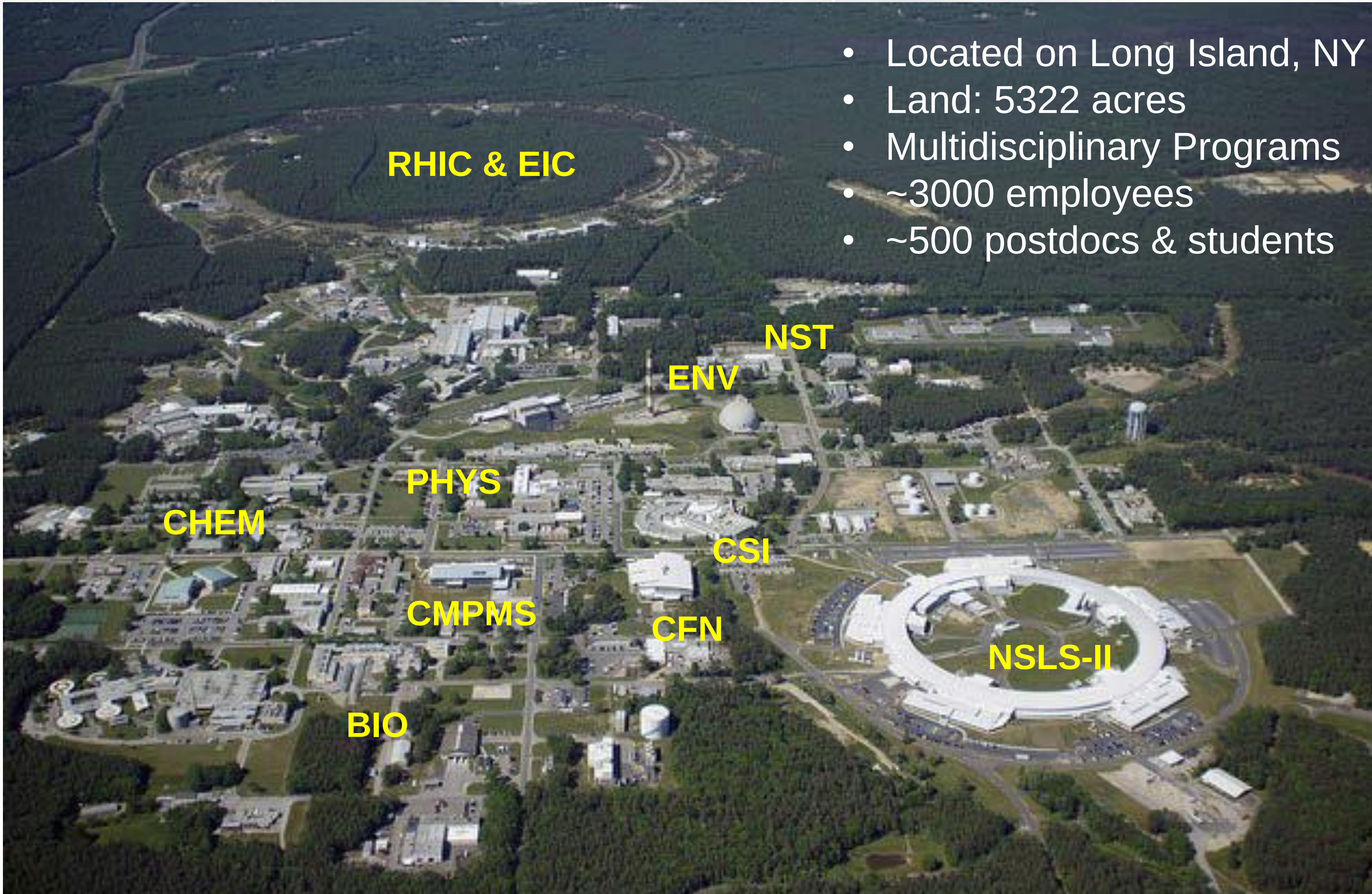

- Located on Long Island, NY
- Land: 5322 acres
- Multidisciplinary Programs
- ~3000 employees
- ~500 postdocs & students

Accelerator and Beamline layout

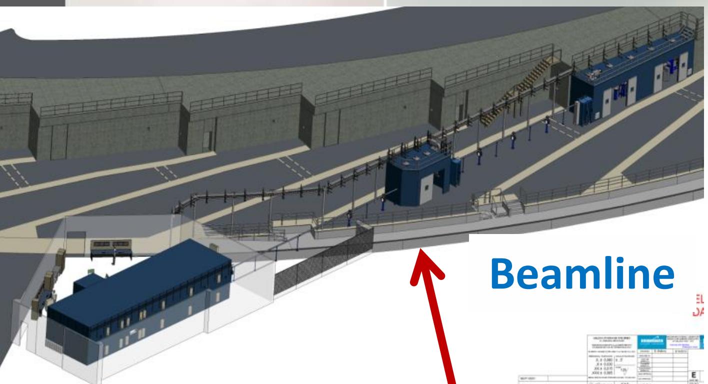

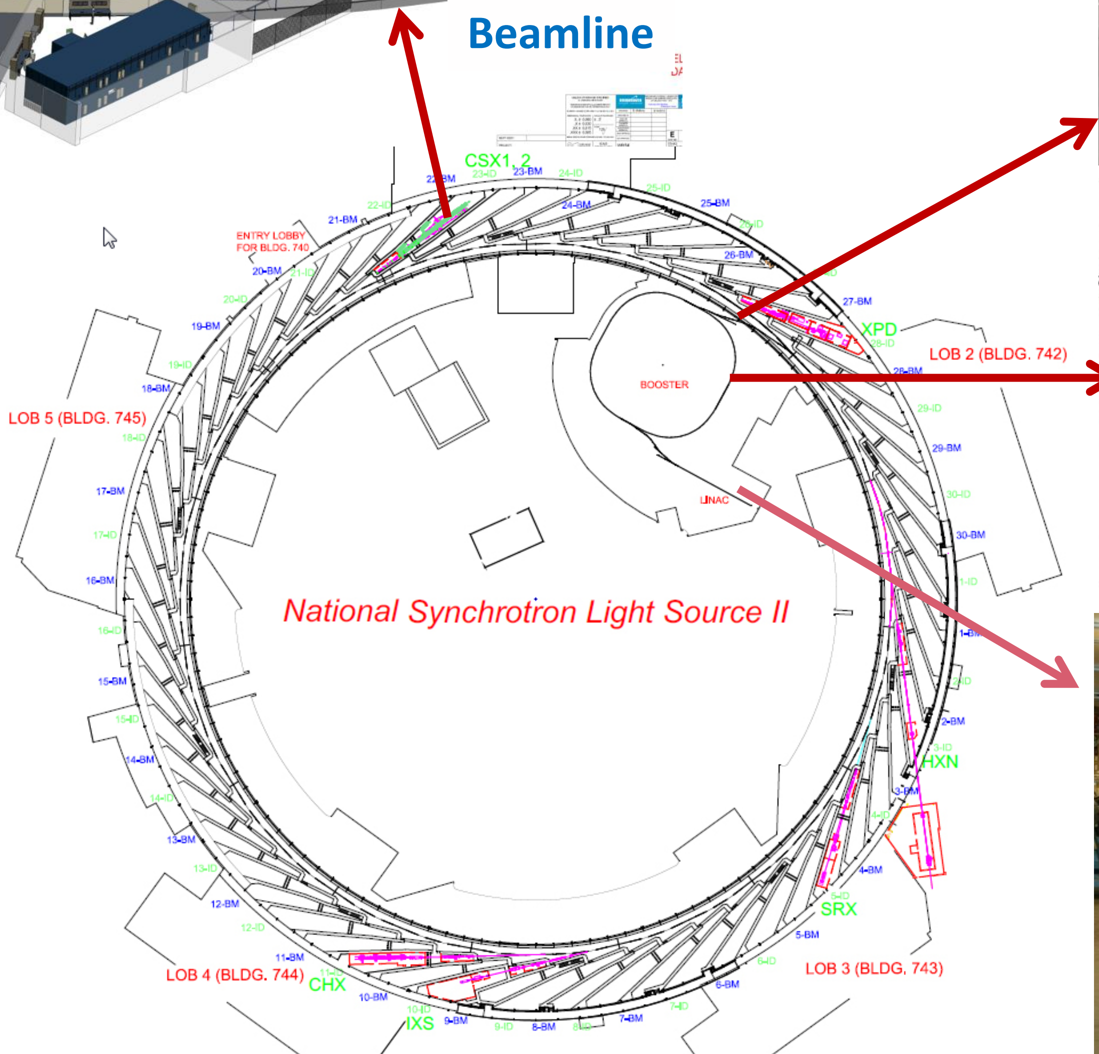

Linac

- 200 MeV linac, built by Research Instruments, GmbH in collaboration with BNL.
- It consists of a DC thermionic electron Gun, bunching system and four 3 GHz TW structures.
- Gun operation modes: SBM and MBM.
- Commissioning activities: Mar. 26, 2012 →Jun. 18, 2012

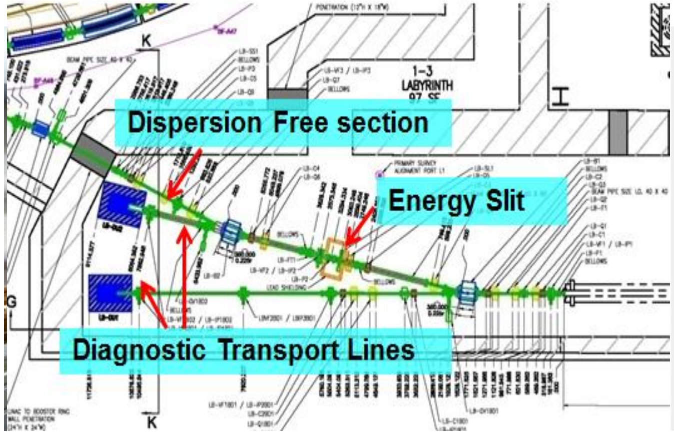

Linac beam Energy Spectrum

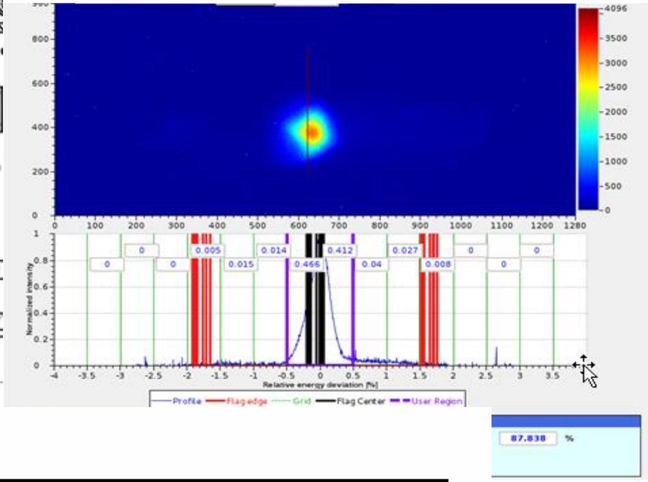

Linac performance

Parameter	Specification		Single Bunch Mode	Multi Bunch Mode
Energy	200 MeV		201 MeV	210 MeV
Charge	>0.5 nC Single Bunch Mode	>15 nC per train Multi Bunch Mode	0.5 nC	11 nC
Bunch Train Length	160 – 300 ns MultiBunch Mode		N/A	160-300 ns demonstrated
Bunch Train Uniformity	<10% MultiBunch Mode		N/A	25%
Energy Spread	<0.5% rms		0.14% FWHM, with 80% of charge within 0.5%	0.41% FWHM, with 72% of charge within 0.5%
Emittance	<38 nm rms - design <70 nm rms - acceptance		X: 58 nm, Y: 63 nm	X: 56 nm, Y: 47 nm

Booster

- Booster circumference is 158 .4m (1/5 of storage ring circumference), four periods of combined-function FODO lattice
- The booster magnetic field and RF voltage are ramped to accelerate the beam from 200 MeV to 3 GeV
- Nominal repetition rate is 1 Hz with possibility to upgrade for stacking and 2 Hz
- At the extraction energy, booster provides low horizontal emittance of 37.4 nm-rad and vertical emittance of ~1 nm-rad

- First beam injection into Booster on Dec. 3rd 2013
- The beam was accelerated to 3 GeV on Dec. 31, 2013.
- The commissioning of the booster was successfully completed in Feb. 2014.

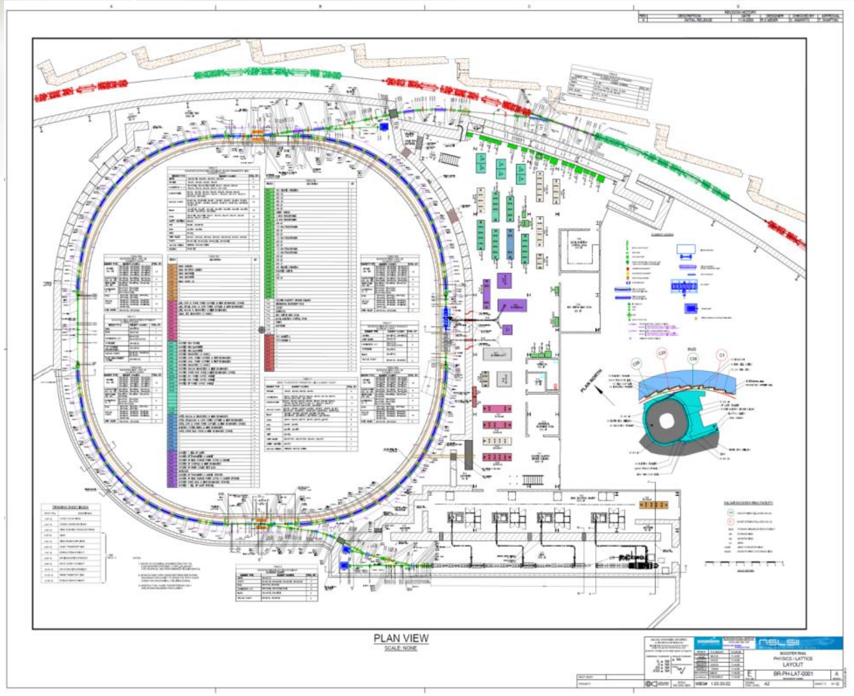

Booster performance

Comparison of Booster Specifications and Measurements

Parameter	Design	Measured
Beam energy	3+/-0.15 GeV	~3 GeV
Bunch charge	0.5…15 nC	0.5…10 nC
Bunch train	1 / 80…160 bunches	1 / 75 bunches
Beam energy spread @3GeV	0.08%	0.10%
Beam emittance X	38 nm rad	33 nm rad
Beam emittance Y	4 nm rad	4…8 nm rad
Charge transport efficiency between ICTs in LB and BSR TL	>75%	~80% as seen between LtB and BsT FCTs

Storage Ring

- 500 mA beam current with 1 nm-rad horizontal and 8 pm-rad vertical emittance
    - Beam sizes at source points are ~100 um/3 um
- 15 long (9.3m) and 15 short (6.6m) straight sections
- 1080 bunches in 1320 RF buckets, 3 hrs lifetime
- High beam stability in position (<10% of rms beam size) and angle (<10% of rms divergence)
- Top off injection for stable intensity (±0.5% variation)
- 28 operation beamlines from diverse radiation sources (DW, EPU, IVU, 3PW, Dipole)

Parameters	Value
Beam Energy [GeV]	3
Circumference [m]	792
Number of DBA cells	30
Number of ID straights	15*6.6, 12*9.3
Beam Current [mA]	500
X/Y Emittance [nm-rad]	1/0.008
Relative energy Spread	0.1%
RF Voltage [MV]	4.9
RF frequency [MHz]	499.68
Energy loss/Turn [keV]	287/700

One super-period SR Lattice function

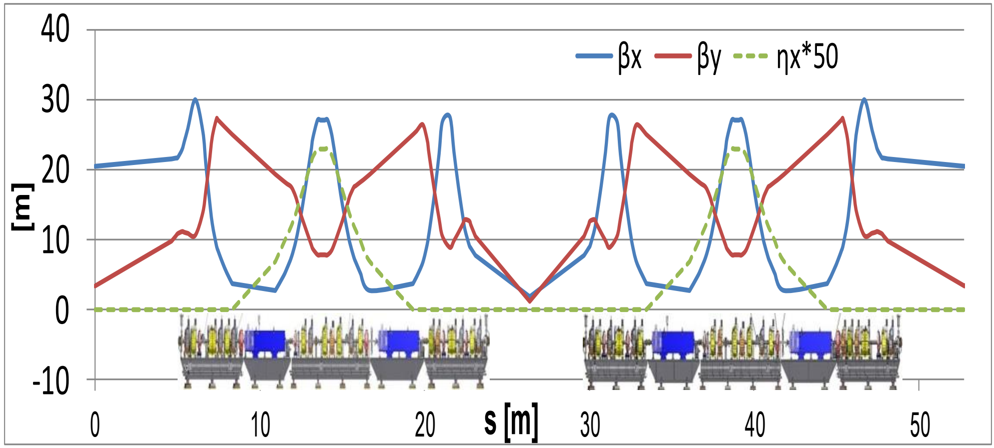

SR Subsystems

- Subsystems: Magnets (900), Power Supply (806), Vacuum system, RF system, Instrumentation, Insertion Devices, Injection system, Water cooling systems, Cryogenic Plant, Controls, Personal Protection System, Equipment Protection System

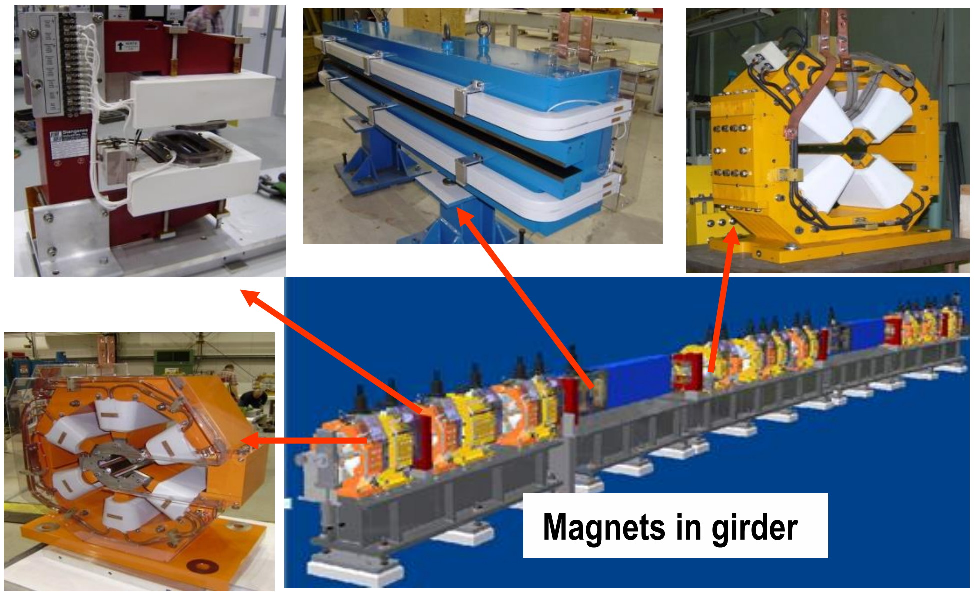

Magnets in girder

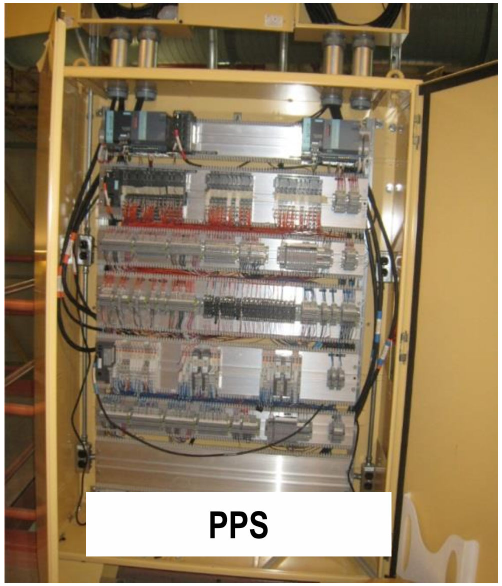

PPS

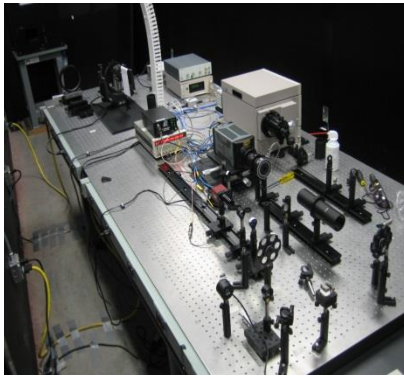

Synchrotron Light Monitor

Beam Positon Monitor Button

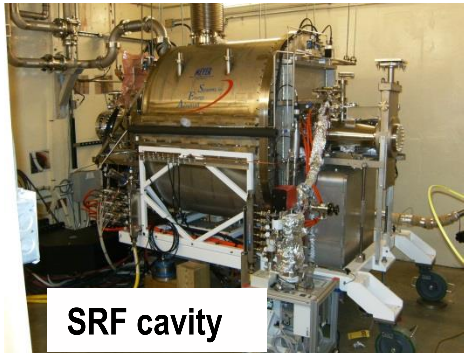

SRF cavity

LN tank

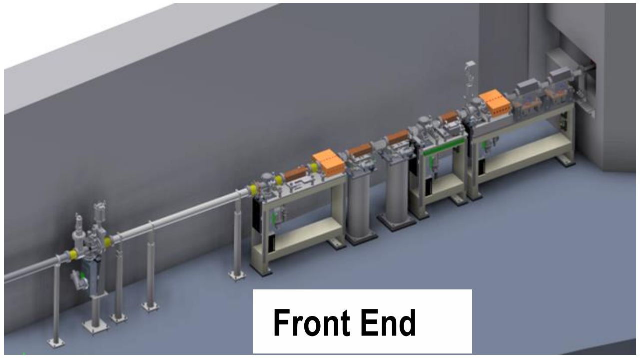

Front End

Insertion devices

BL	ID straight type	ID type, incl. period (mm)	Length	K_{max}*	FE type†	FE aperture (h x v, mrad)	# of ID's (base scope)	# FE's	Project	Procurement
CSX	lo-β	EPU49 (PPM) x2	4m (2 x 2m)	4.34	canted (0.16)	0.6 x 0.6	2	1	NSLS-II	Done
IXS	hi-β H	IVU22 (H) (x2)	6m (2 x 3m)	1.52	std	0.5 x 0.3	1	1	NSLS-II	Done
HXN	lo-β	IVU20 (H)	3m	1.83	std	0.5 x 0.3	1	1	NSLS-II	Done
CHX	lo-β	IVU20 (H)	3m	1.83	std	0.5 x 0.3	1	1	NSLS-II	Done
SRX	lo-β	IVU21 (H)	1.5m	1.79	canted (2.0)	0.5 x 0.3	1	1	NSLS-II	Done
XPD	hi-β H	DW100 (H)	6.8m (2 x 3.4m)	~16.5	DW	1.1 x 0.15	0	1	NSLS-II	Done

Damping wiggler

3PW

IVU22

T.Tanabe

Machine Performance: Beam emittance

- Beam emittance
- Beam stability
- Operation reliability
- High current

Emittance: photon Brightness/Coherence

- Electron beam emittance

$$\varepsilon_x = \sigma_x \sigma_{x'} \quad \varepsilon_y = \sigma_y \sigma_{y'}$$

- Total source emittance

$$\bar{\varepsilon}_x = \sqrt{\sigma_r^2 + \sigma_x^2}\sqrt{\sigma_{r'}^2 + \sigma_{x'}^2}$$

- Photon brightness

$$B = \frac{F_n}{(2\pi)^2 \bar{\varepsilon}_x \bar{\varepsilon}_y}$$

- Coherent flux fraction

$$P_c = \frac{F_c}{F_n} = \frac{\lambda^2}{(4\pi)^2 \bar{\varepsilon}_x \bar{\varepsilon}_y}$$

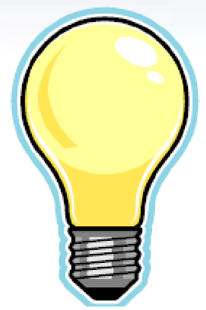

Low Brightness

High Brightness

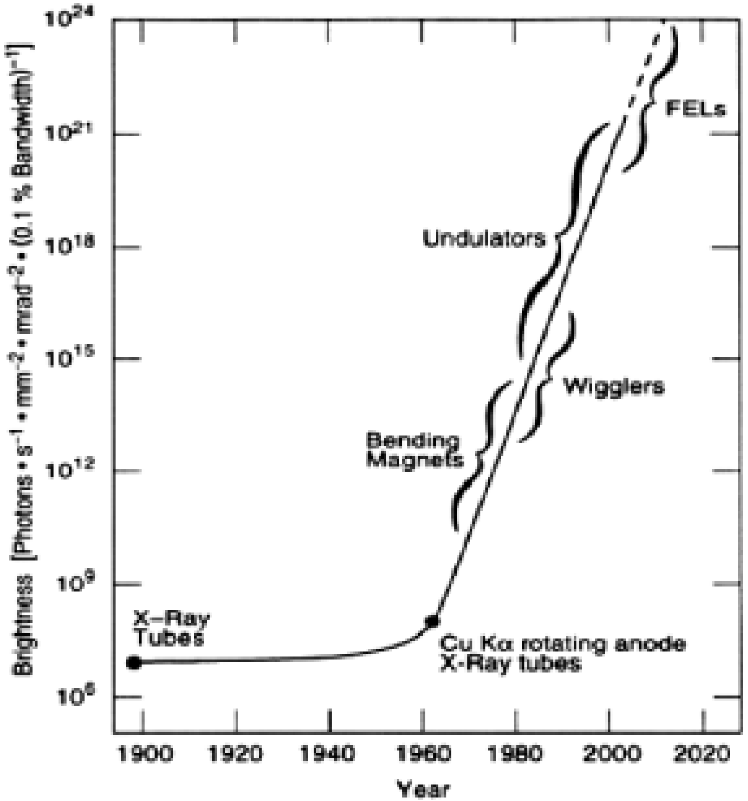

Horizonal beam Emittance

- SR equilibrium horizontal emittance is determined by radiation damping and quantum excitation: $\varepsilon_x = C_q \frac{\gamma^2}{J_x} \frac{I_5}{I_2}$
- 30-cell DBA producing the horizontal emittance of 2 nm-rad
- Three Damping Wigglers further reduce the beam emittance to half by adjusting the synchrotron radiation integrals

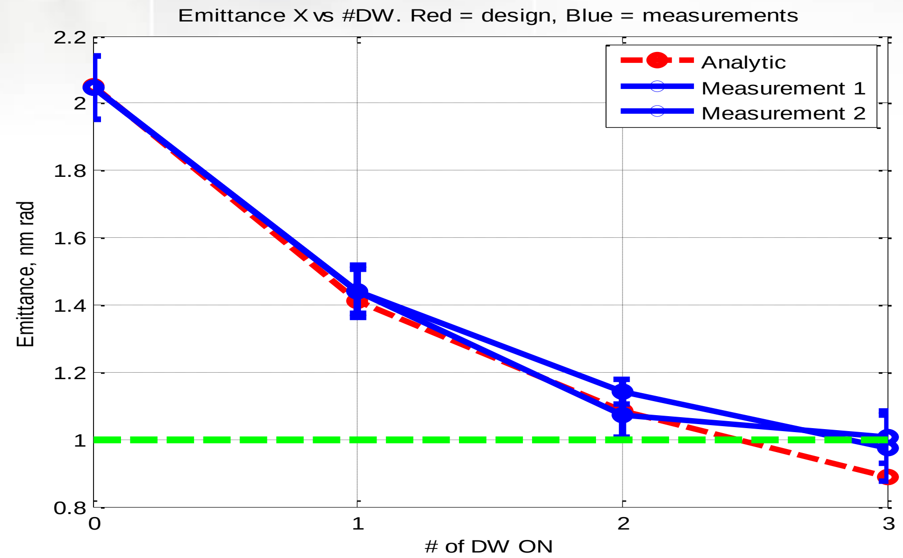

- **Design Emittance Achieved**

ε_x^{0dw} = 2.05 nm·rad, ε_x^{3dw} = 1 nm·rad,

ε_y = 7 pm·rad, exceed diffraction limited value of 8 pm-rad (at 10 keV), which also was verified by HXN x-ray beam image size (change by 33%)

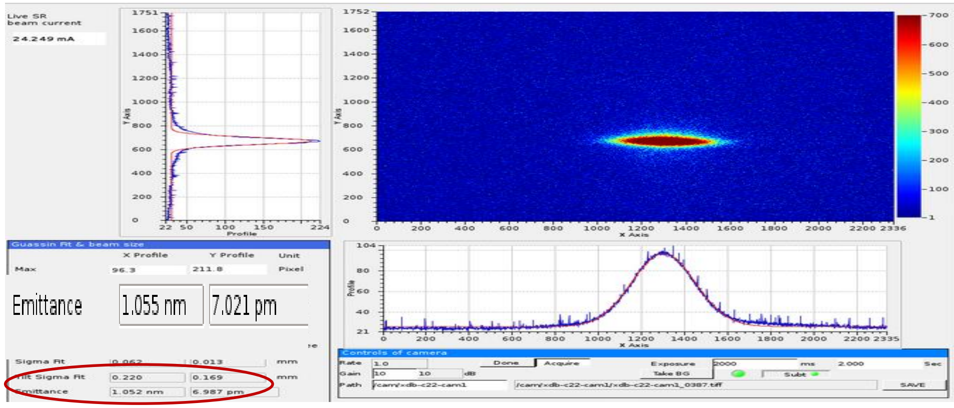

Vertical beam emittance

- Routine operation at 30 pm vertical emittance
- 8 pm diffraction vertical emittance: correct vertical dispersion and betatron coupling by skew quads
  - Electron beam size and divergence decrease by a factor of 1.7
  - Beam life is shorter, from ~8 hrs to ~4 hrs at 375 mA
  - Top off injection more frequently, from 140 second to 90 seconds per shot
- Vertical beam emittance impacts on beamlines performance
  - CHX: Interference patterns show a significant increase in the visibility/contrast with smaller emittance
  - HXN: observed 25% increase (VS model 45%, not fully benefit) in peak intensity, but beam stability degradation

CHX interference pattern

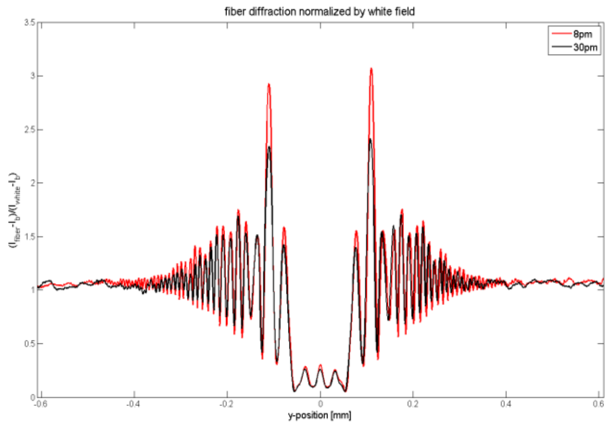

HXN intensity and image

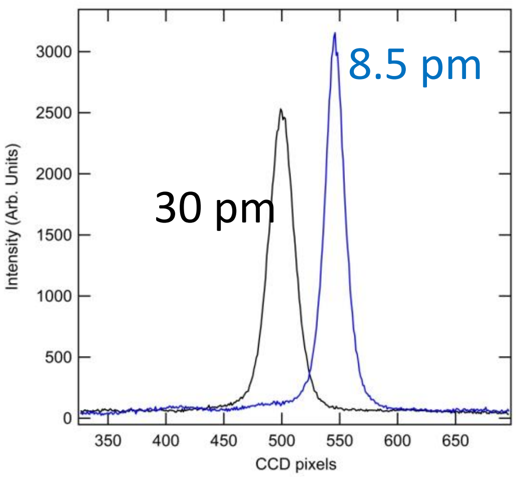

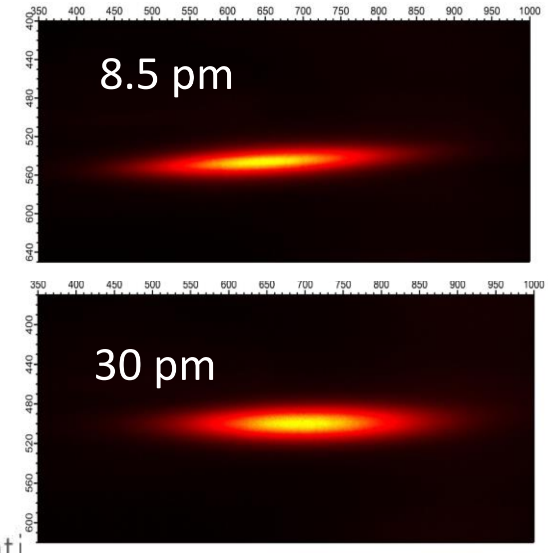

Machine Performance: Beam stability

- Beam emittance
- Beam stability
- Operation reliability
- High current

Beam Short-term Stability with FOFB

Power spectrum density

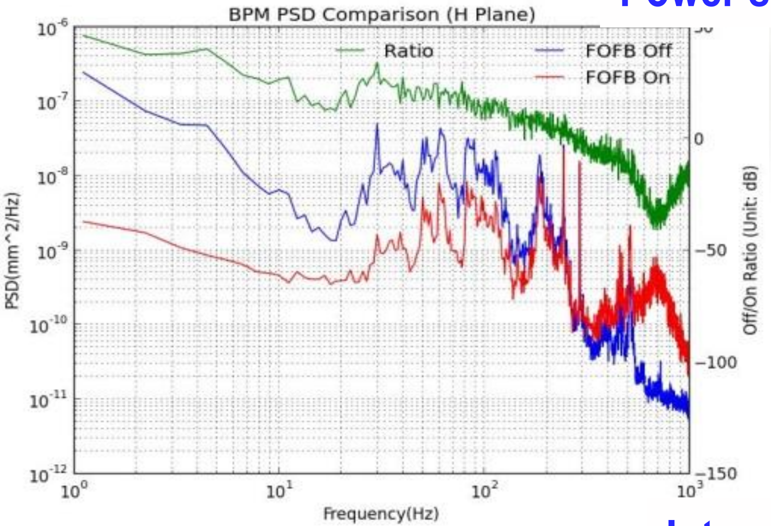

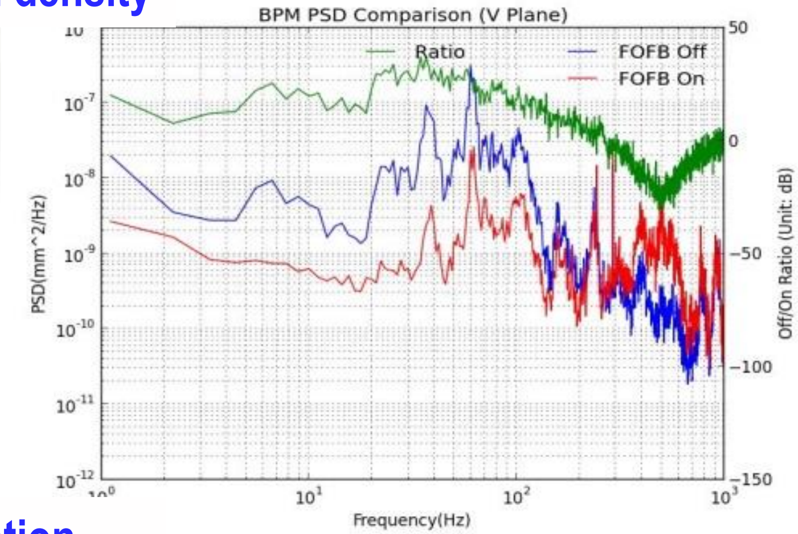

Integrated motion

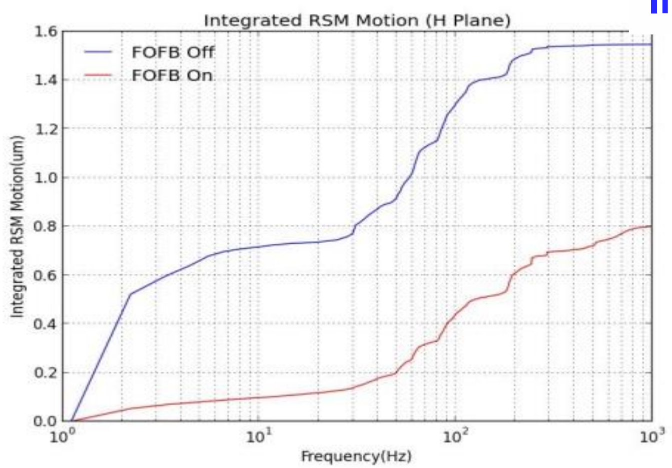

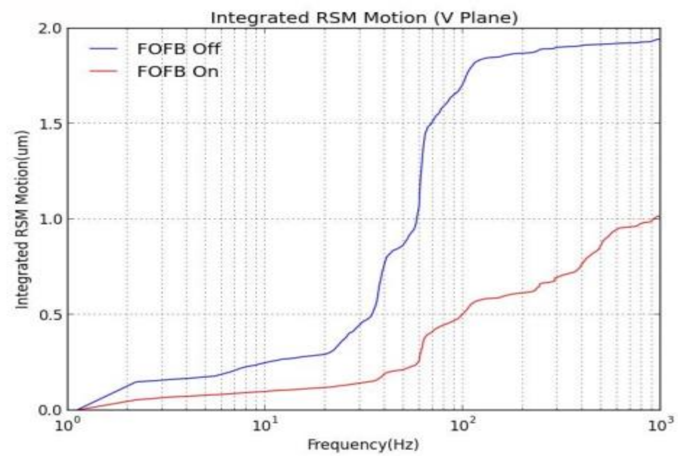

- FOFB (Operation from June 2015 and continuously improved): 90 Fast correctors + BPMs 10 kHz data (120 arc non-dispersion BPMs + ID BPMs)

Beam Short-term Stability with FOFB

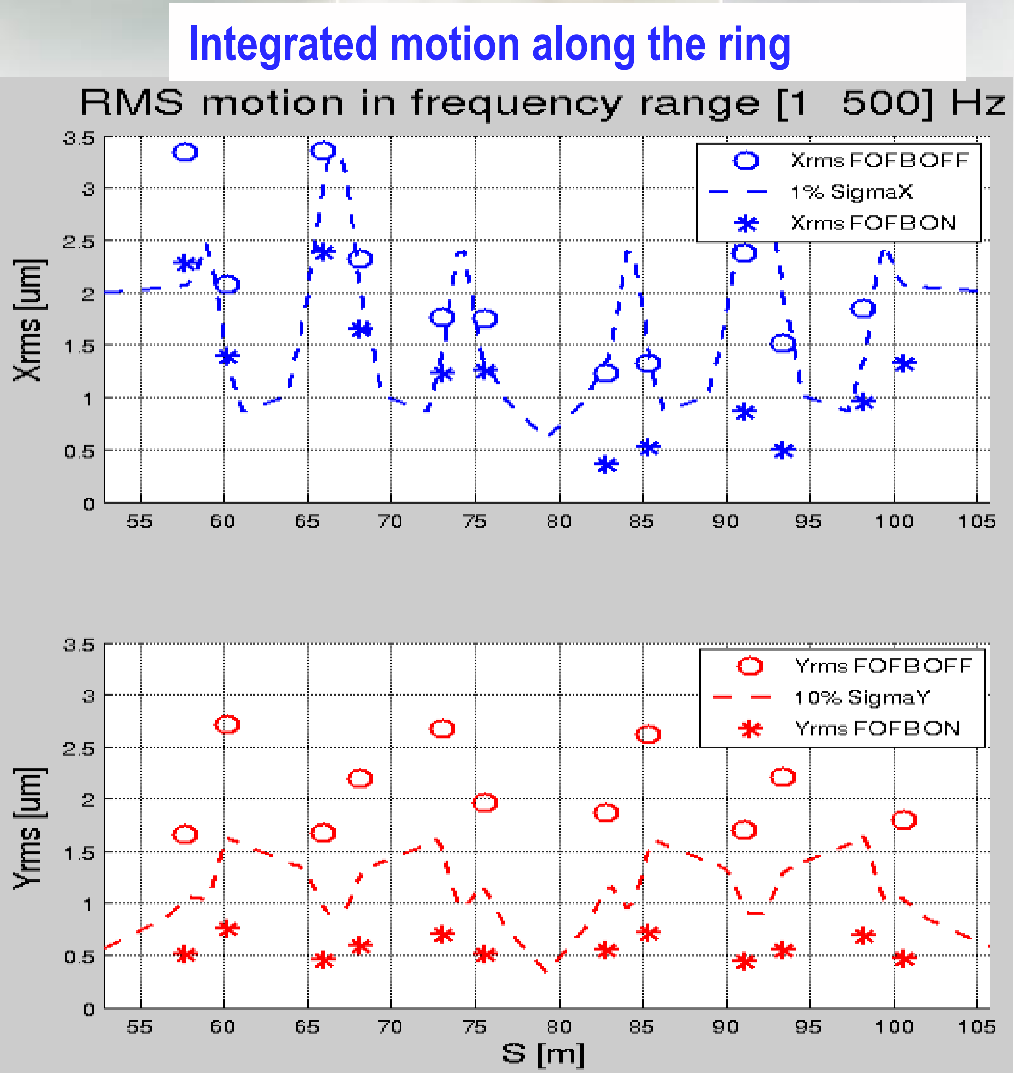

- Beam orbit stability specification: 10% beam size
- Measurement of stability: 1% Horizontal beam size, ~ 10% Vertical beam size

Nati *Y. Tian, L. Yu, W. Cheng*

Beam Long-term Stability: RF Frequency feedback

- Bending magnet/3PW photon source sample data collection can last over 10s hours and long term stability is critical to get high quality imaging
- SR circumference daily change can cause BM photon source ~50 μm, which cannot be corrected with FOFB
- RF frequency feedback was implemented to suppress beam long term drift
- BM source long term stability<10% beam size

BM stability w/o RF freq. FB

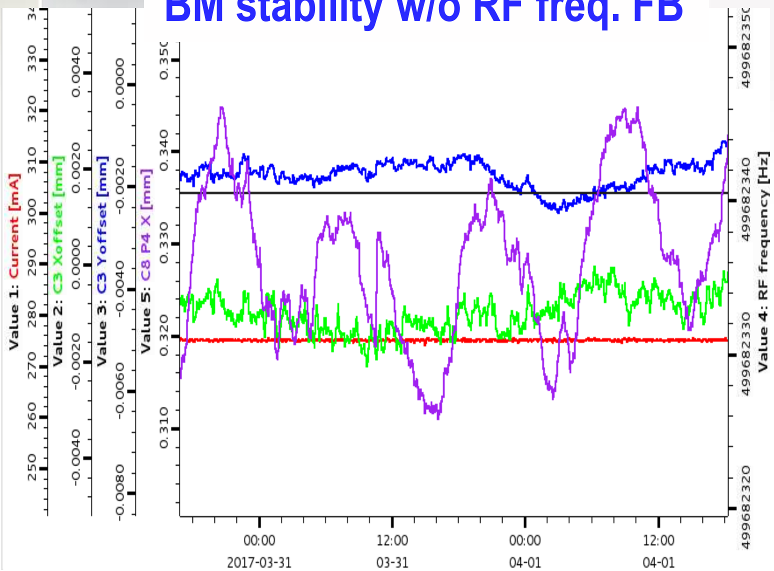

TES bending magnet beamline

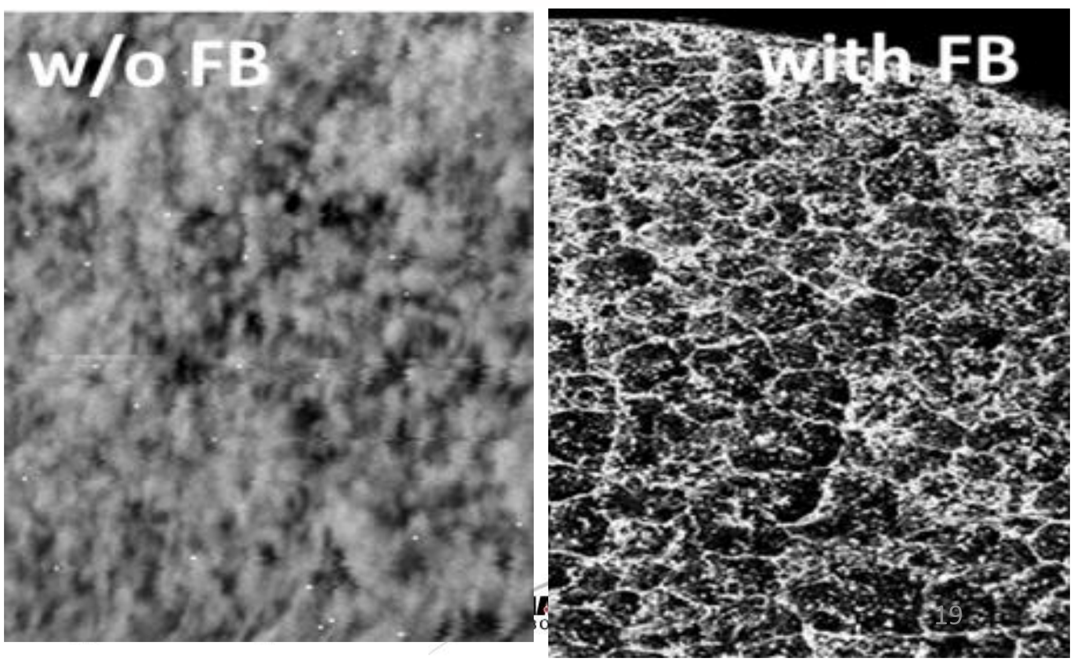

BM stability with RF freq. FB

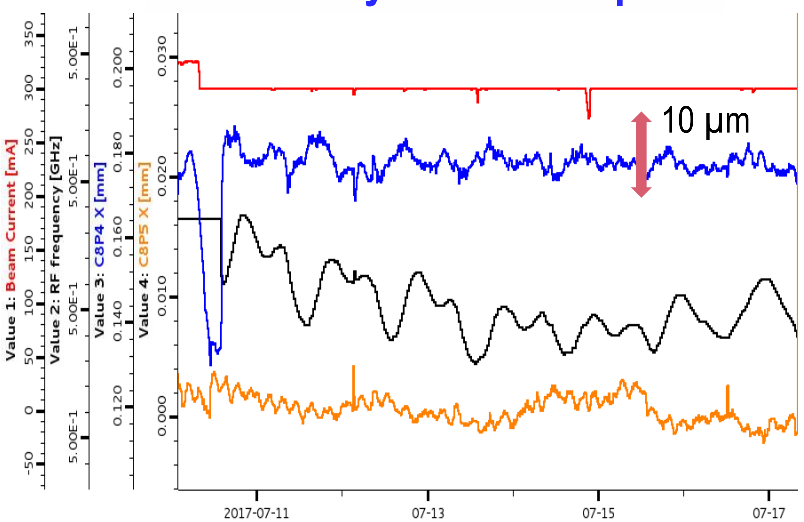

Machine Performance: Operation reliability

- Beam emittance
- Beam stability
- Operation reliability
- High current

NSLS-II: 6 years operations

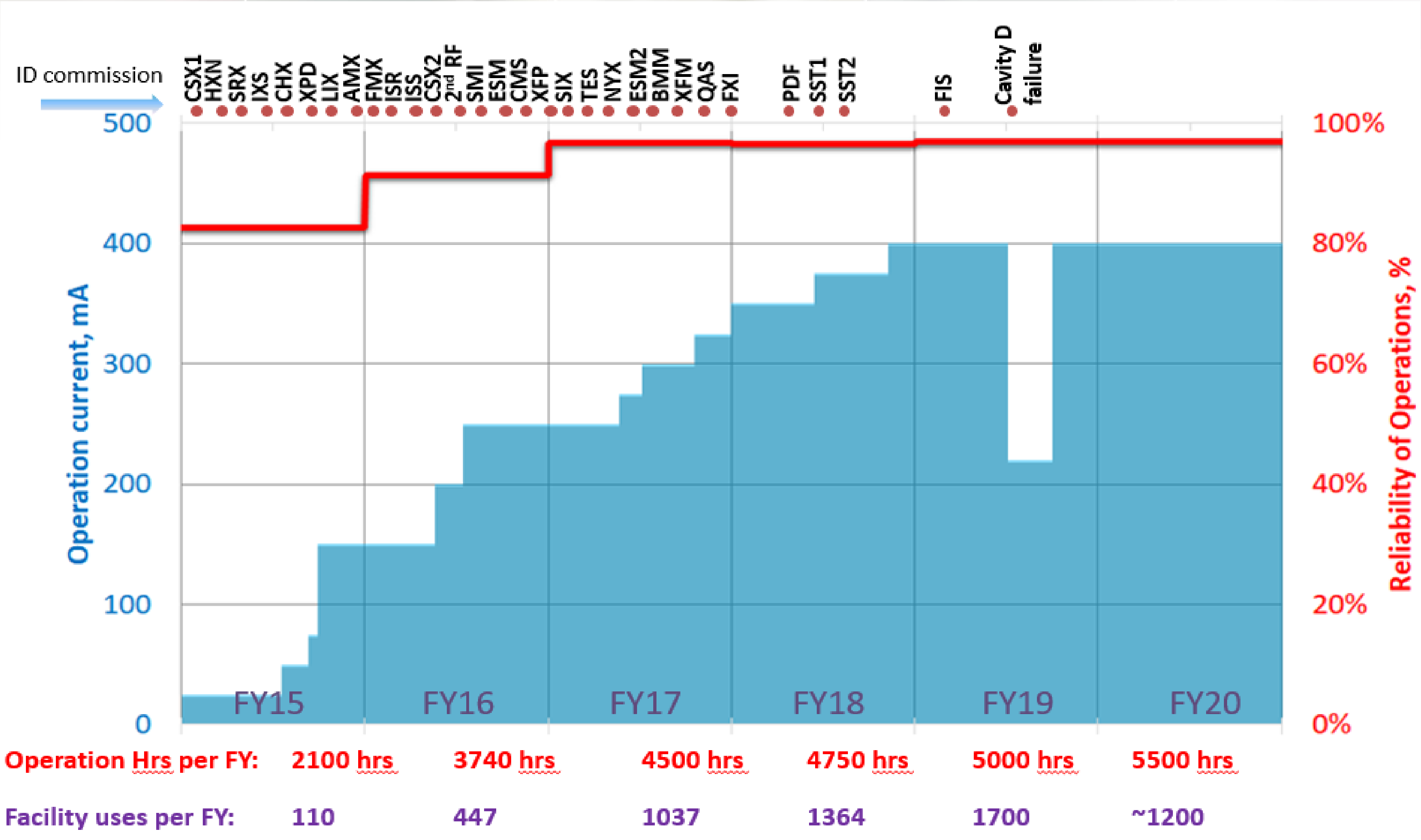

- Commissioned 29 IDs sources (10 IVUs, 6 EPUs, 6 DWs, 5 3PWs, 1 BM and 1 PU)
- High reliability has been maintained while we steadily increased beam current & IDs
- Normal operation with 2 cavities limits our performance (max 400 mA)
- Forced to decrease ops current to 220 mA due to the failure of one cavity in Apr. 2019

FY20 Q4 Accelerator Reliability

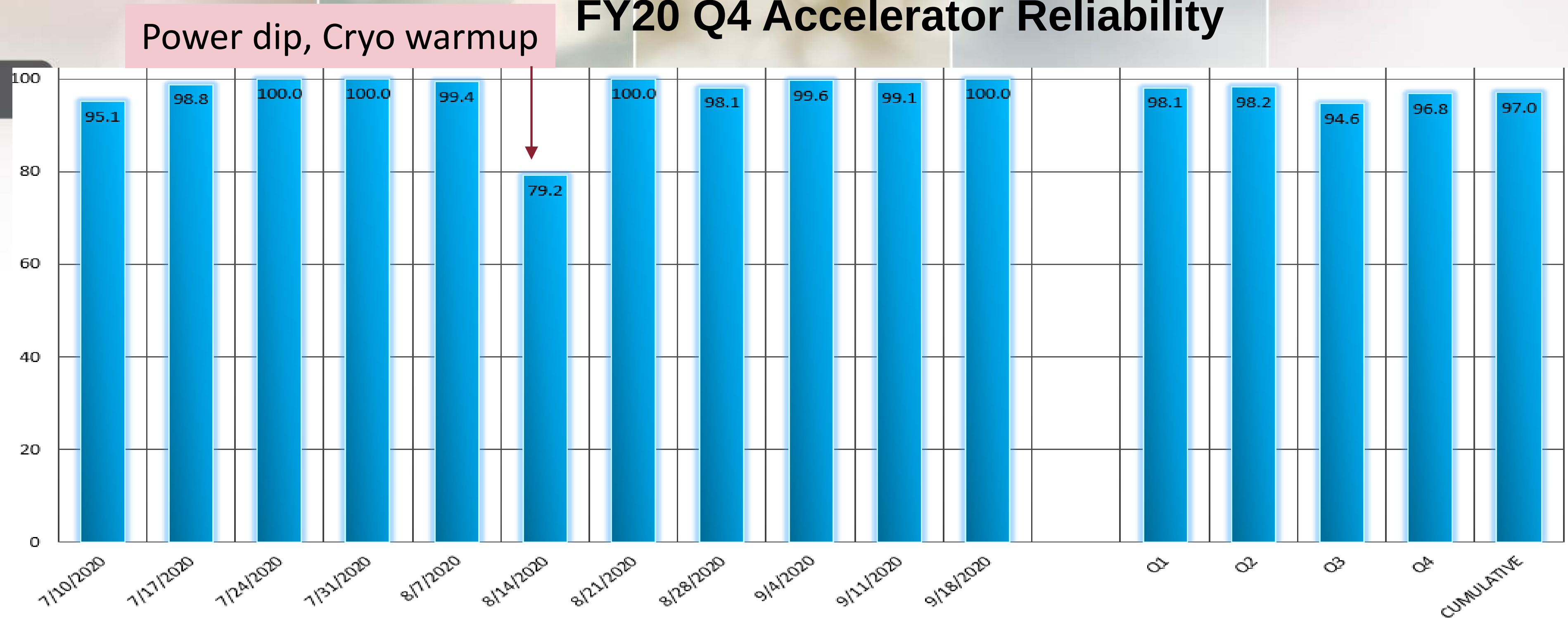

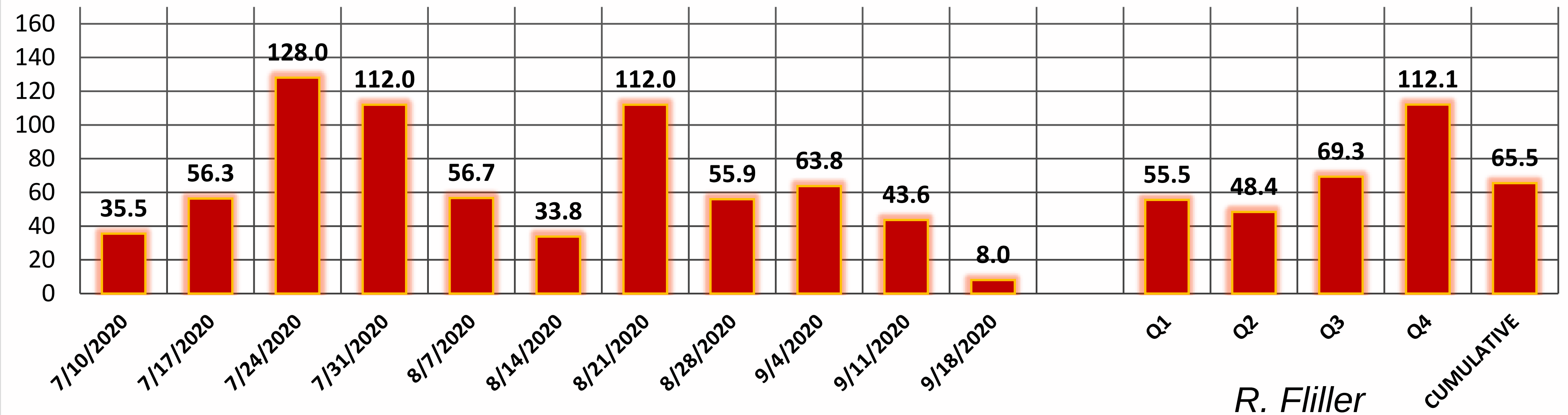

R. Fliller

Operation reliability

- Weekly review beam dump sources and machine down time. Evaluating fault reports and subsequent corrective actions.
- System and component failures
  - Review lessons learned and formalize standard response (Cryo problem, water leak in tunnel),
  - After hours faults. All groups provide phone or online support and will return to BNL to rectify problems when needed. Floor Coordinators trained to replace Klixon panels, troubleshoot with system expert support, reset ion pump controllers, reset ID drive controllers, reset dipole power supply with system expert support, relieve helium pressure at valve box)
- Maintenance activities: two days/~3 weeks
  - Work Requests are generated for all tasks, reviewed by WCC and all groups at maintenance meetings prior to maintenance period
  - Approve, Track, Confirm “Ready for operations” and close all jobs
  - Spreadsheet based with emails→ *online work request under development*
- Recurring problems (identification and corrective action)
  - Ground currents (Regular inspection and repair)
  - Reduced water flow in magnets (alarms, regular thermal inspection and repair)
  - BPM faults (incorporated glitch filter to prevent related faults)
  - RF Trips (Pump and purge, Partial warmup of RF cavities)
  - ID/FE shutters (inspect and reposition shutter switches, train BL staff to delay opening doors)
- Tracking subsystem performance trend: Spare parts
  - Identification, tracking and requisition approval
  - Current list has 2255 items, includes consumables (348), investments (1899) and equipment (8)
  - Prioritize by impact due to failure, quantity in service, lead time, expected life and cost
  - Spreadsheet based with emails
- Developed EPICS control system for NSLS-II primary water utility system, accelerator and beamline Personal Protection System (PPS): utility performance trend, water leak monitor, FE water flow drift monitor
- Developed HLA common tools and cross training accelerator physicists

L. Doom

Post mortem function: beam dump analysis

- Various sources (AI protection system or subsystem malfunction) may cause beam dump
- Post mortem function: capture the sub-systems status and beam information during beam dump, including RF system, power supply, BPMs and active interlock system. Data is used to analyze subsystem trip sequence
- Beam dump sources: RF Cavity, PSs, AI, IS kicker, EPS, PPS...

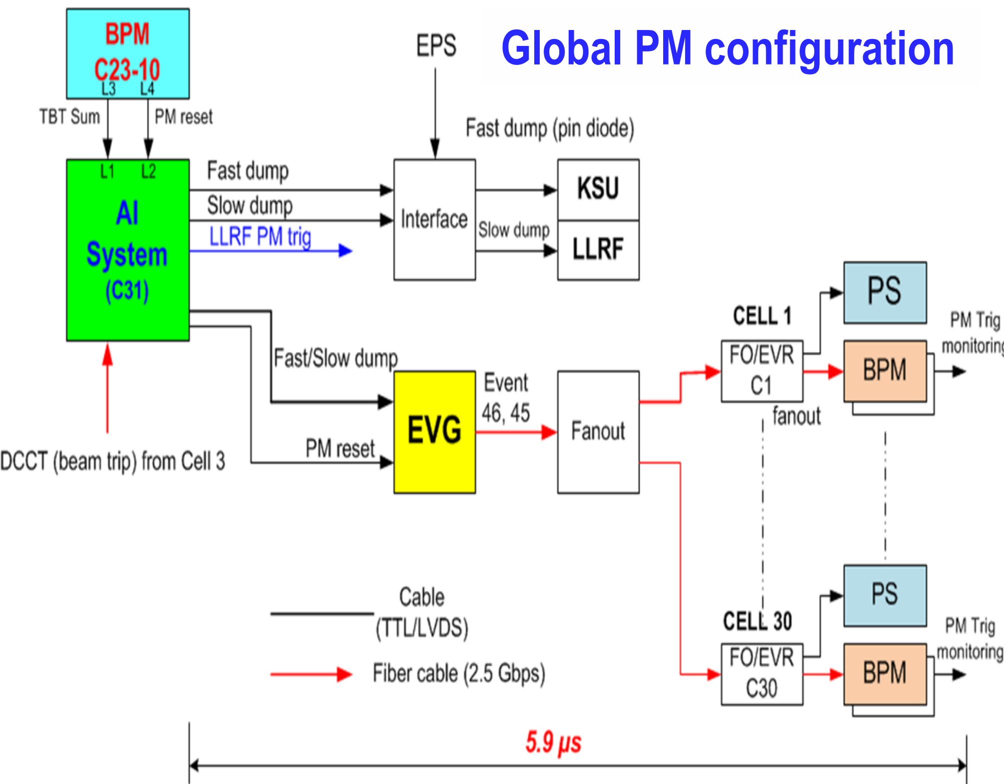

Example of beam dump source: RF trip

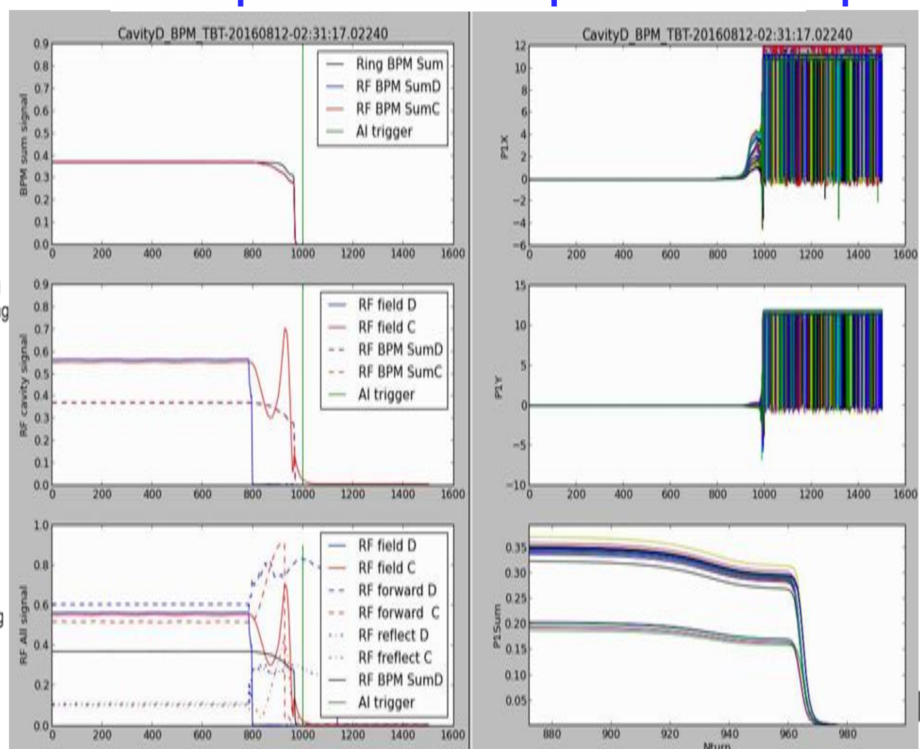

Subsystems with the Highest Impact on Downtime

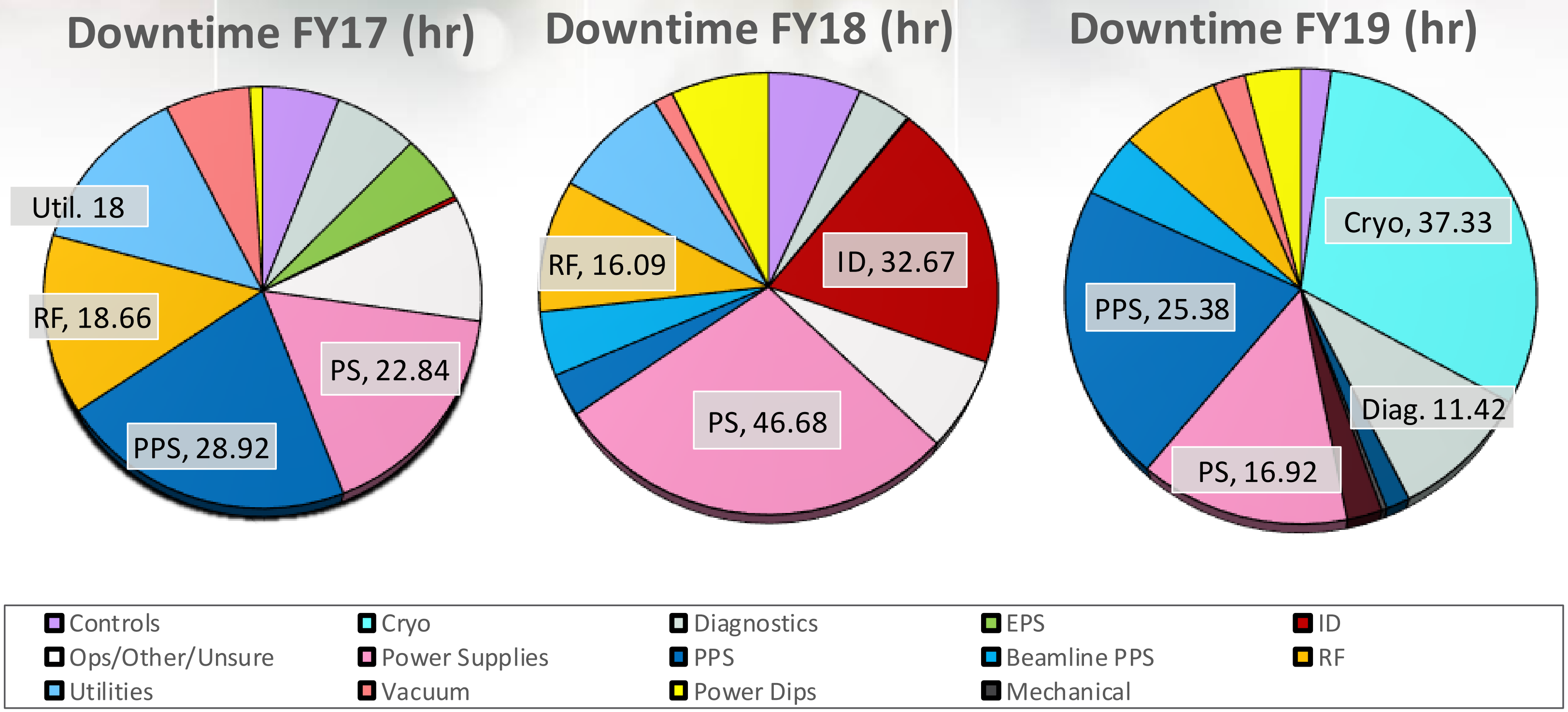

- Main contributors to machine downtime are from RF, Cryo Plant, Utilities, Power Supplies
- RF: 111 trips and 87 hrs downtime in FY16 due to cavity D vacuum and field instability
- Lost RF cavity C in 2019 → 3.5 months of operations to low operation current
- Cryo Plant: cold box warm up ~monthly after burst disc event in June 2017
- Utilities: cooling water quality caused an increase in ground current faults and trips due to magnet overheating, required ~5 hrs to flush
- Power Supplies: majority of FY18 downtime due to single booster PS event

Cryoplant Problems and Ongoing Improvements

- Burst disc event in June 2017, caused by carpenter accidently bumping an E-stop(!) contaminating helium in cryo plant
- Cold box warm-up and Pump & Purge
  - 16 times over two years
  - 2 of them required unexpected secondary warm-ups that resulted in significant downtime
- Typical warm-up takes about 2.5 days with around-the-clock expert support

Burst disk rupture contaminates cryoplant

Improvements

- Additional helium storage tank to increase inventory
  - Allow longer cold box maintenance while keeping cavities cold
- Fixed three helium leaks on low pressure suction lines
- Full flow helium purifier
- Replaced Pressure Relief Valves on cavities
- Need a fully spare cryoplant

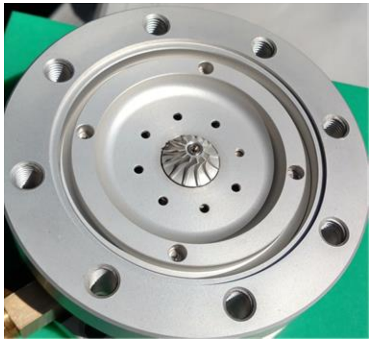

Contamination fouls 340,000 rpm turbine

Utilities system

Copper Corrosion

- a serious problem for the accelerator system:
  - High DI water resistivity
  - High levels of dissolved oxygen
- Problems caused
  - Clogging of magnet water circuits
  - Increased magnet temperatures
  - Increased ground currents

Buildup on water channels in manifold blocks

Improvements

- Cleaning/flushing magnet assemblies
- Install De-aerating system to lower O2 level
- Upgrade to optical dissolved oxygen sensors
- Lower resistivity setpoint
- Regular monitoring of ground currents
- Installation of digital temperatures sensors on magnet coils and regular monitoring
- Clogging and ground currents have been significantly reduced.

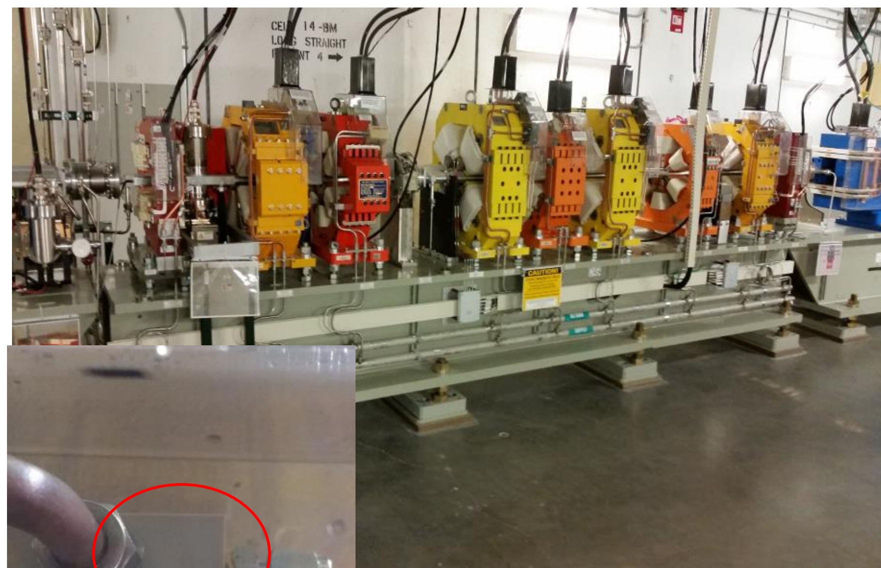

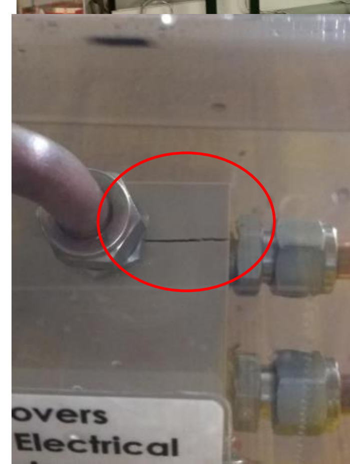

Water leak due to Magnet cracked manifold

L. Doom

Machine Performance: High current

- Beam emittance
- Beam stability
- Operation reliability
- High current

History of high current studies

Date	Current	Operation condition and notable issues
Apr. 29, 2014	25 mA	Normal RF cavity
Jul. 11, 2014	50 mA	1st SC RF cavity
Mar.,2015-Jul. 2015	100-300 mA	IDs open, no issues observed
Feb. 16, 2016	375 mA	2nd SC RF cavity in operation. Ceramic chamber temp. reached 94 ^{o}C in one hour
Apr. 18, 2016	400 mA	Ceramic chamber temp. 110 ^{o}C with lower RF voltage
Jun. 2016-Nov. 2017	7 more 400 mA studies	Identified hot spots. Varied beam condition: peak current(more bunches), bunch length(3DWs, low RF voltage). Developed and replaced ceramic chambers, RF springs. C11 G4 area vacuum leak
Jun. 30, 2018	425 mA	No issues observed
Aug. 2018-Feb. 2019	450 mA	5 studies: C28 ID area vacuum leak, installed RTDs, replaced RF springs
Feb. 22, 2019	463 mA	Vacuum activity issues, could not reach 475 mA
Mar. 15, 2019	475 mA	Vary bunch filling pattern. Heating at C3 G4 upto 80 ^{o}C
Oct. 7, 2019	500 mA	Partially close IDs

- Multiple sources of heating due to low quality of ceramic coating, deficiency in installation of RF springs, were identified and fixed
- Great progress in increasing beam current since commissioning
- Demonstrated the designed beam current 500 mA

Ceramic chambers

- SR ceramic chambers: 4 fast kickers for beam injection (critical) and 1 pinger for beam dynamics studies
- Require Titanium coating 2 µm thickness over the entire inner surface with ± 10% uniformity

Issues

- Observed heating and vacuum activity during first high current studies in Feb. 2016
- Kicker chamber 2 reached > 100 ^oC @ 400mA. Discovered Titanium coating flaked off and chamber discolored
- Due to limited space, RTDs were installed at the end of chambers to monitor temperature
- High uneven localized heating or abrupt temperature changes
- Chamber failure can cause two days downtime

2016: Ceramic chamber temperature

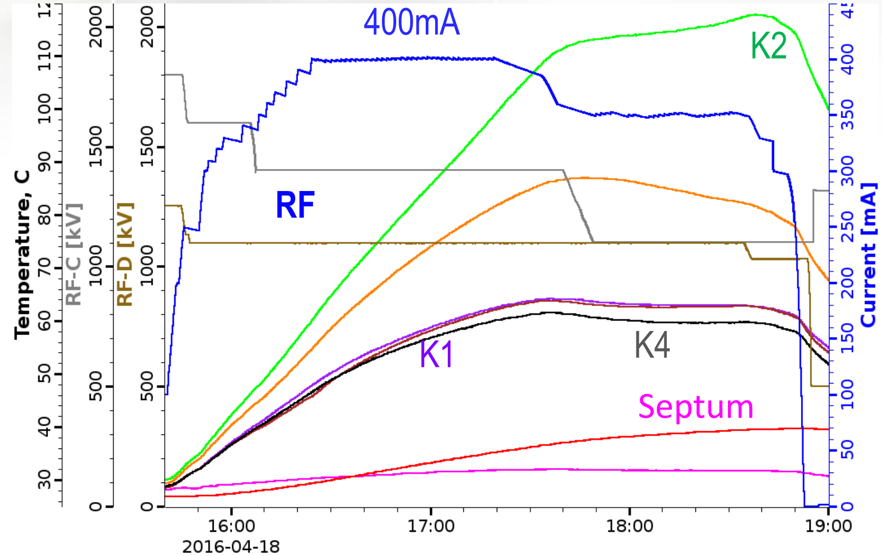

Damaged Kicker 2 chamber

Ceramic chambers

Improvements

- Replaced damaged kicker chamber
- Installed cooling system
- Replaced RF springs between flanges and bellows
- Installed IR camera to monitor heat distribution
- Procured 5 new ceramic chambers and applied Titanium coating in-house. Installed three chambers in May. 2017-Sep. 2018
- Ceramic Temperature reduced to ~40 ^{o}C@400 mA

In-house coating development

- DC magnetron sputtering
- Central anode to initiate discharge
- Integrated thickness monitor
- New coating method successfully improved ceramic chamber thermal performance in operations

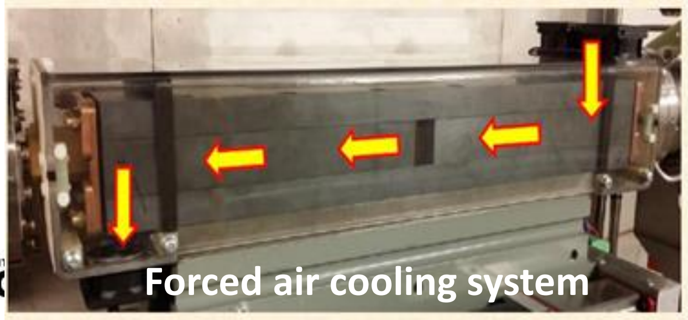

2019: Ceramic chamber temp.

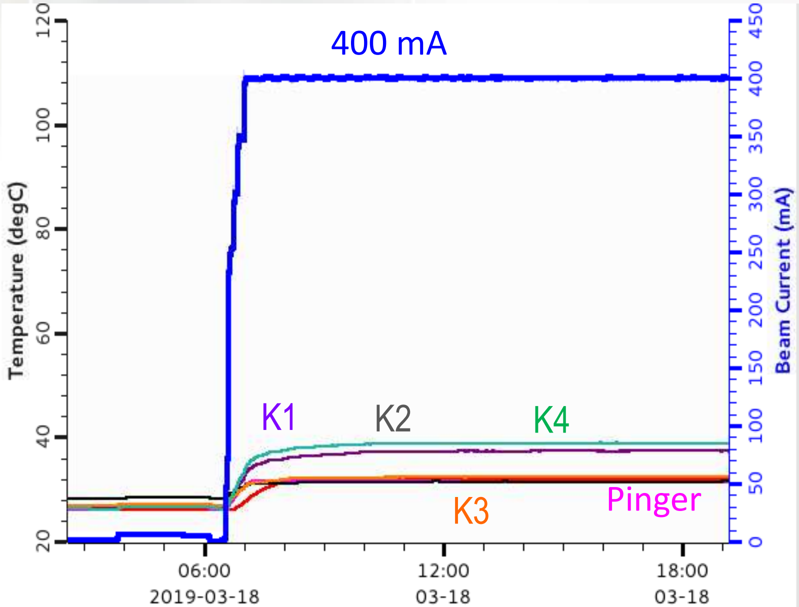

Ceramic chamber coating system

RF springs

- 770 RF Springs installed in Storage Ring

Issues

- Certain temp. sensors indicated temperature > 80°C
- Improper RF spring installation caused trapped mode heating
- Temp. sensors installed at discrete locations do not show all hot spots

Improvements

- In-situ thermal survey
- Installed IR cameras to monitor heat distribution
- Developed new RF spring installation procedure
- Replaced 39 RF springs since 2017 to reduce heating
- Installed 600 new sensors at flanges

Before: with RF springs improperly installed

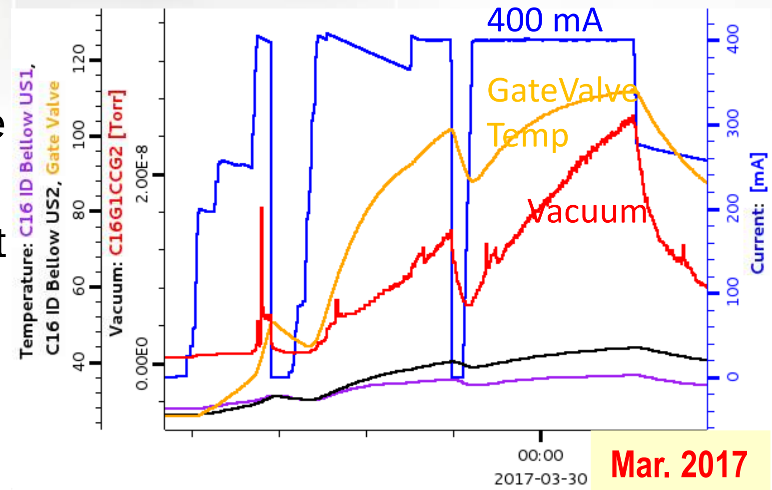

After: RF spring installed properly

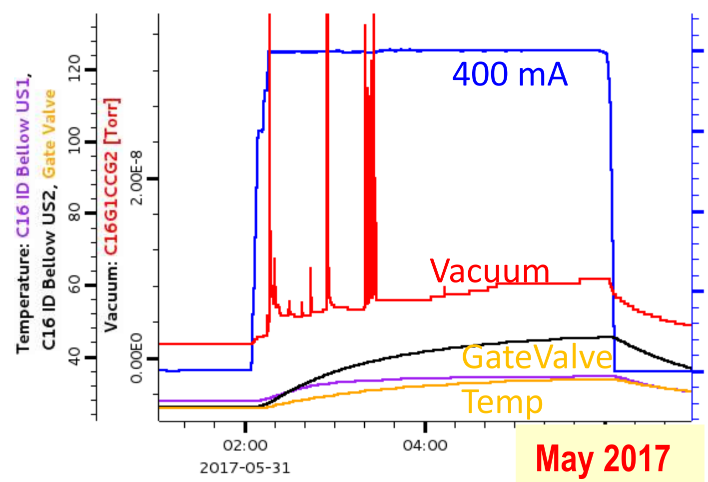

Improper installation of RF springs

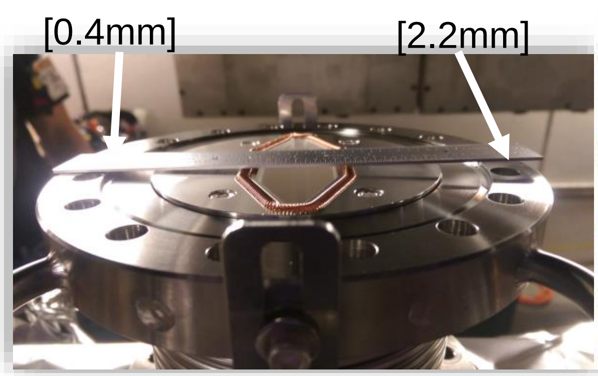

C16 temp. with IR camera

500 mA demonstration

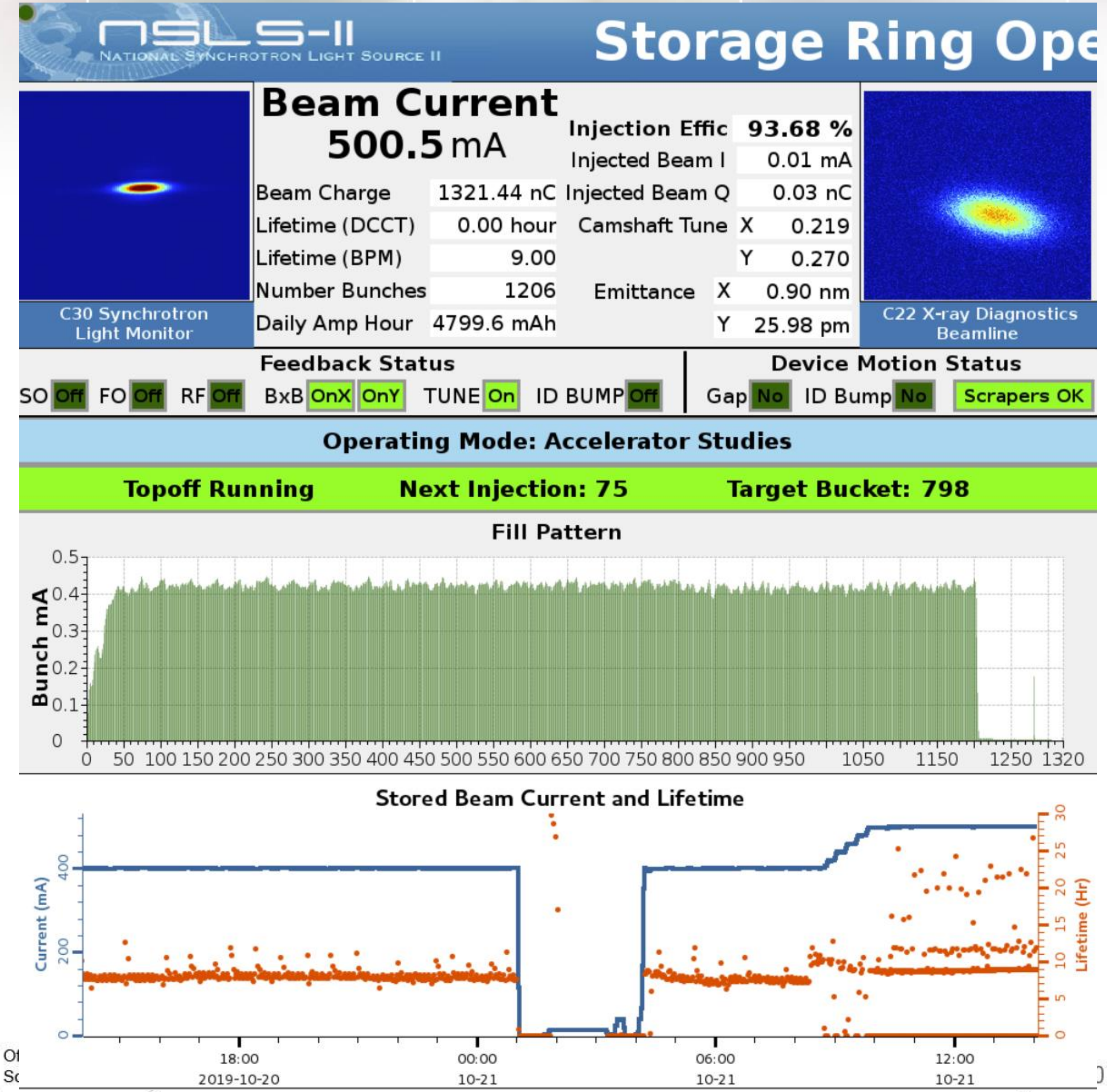

Developments required to reach 500 mA 8pm in operation

4 RF systems: sufficient for compensating power loss of all operating IDs + new (HEX, MIE) @500 mA and provides with redundancy

Third Harmonic Cavity (THC):

- Bunch lengthening: increase bunch length by a factor of 2.5 including gap in bunch train and bunch lengthening effect (3.5 for ideal case)
- Increase beam lifetime
  - Lifetime will double, from 3 hrs to 6 hrs at 500 mA
  - Less frequent top off injections: from 1 to 2 minutes between shots
  - Benefit injector components lifetime: Booster main power supplies, pulsed power supply, etc.
- Lower heating
  - Power loss reduces by a factor of 2.8
  - The ceramic chamber and bellows temp. will reduce with THC

Bunch length and lifetime w/o HC

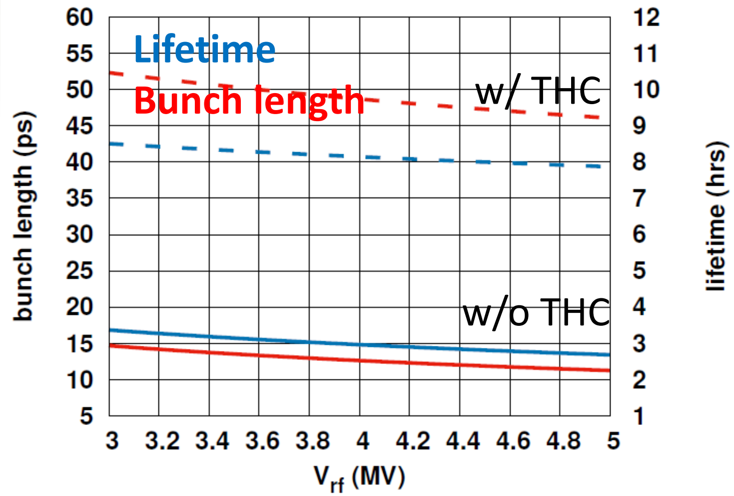

Heating w/ and w/o THC

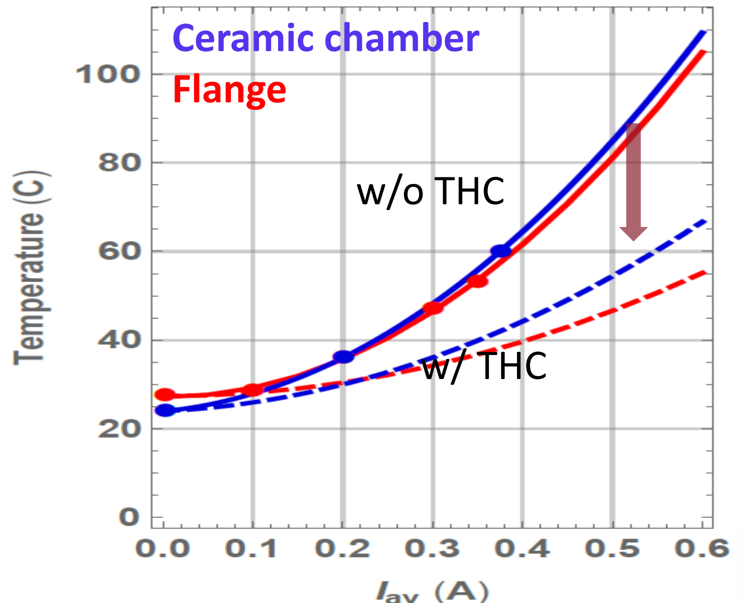

Facility development and upgrade

Mature operation of 500 mA and 8pm

- RF system
  - 3rd RF system sufficient for 500 mA power, to commission in FY21
  - 4th RF system necessary for redundancy
- Harmonic cavity for bunch lengthening
  - Increase beam lifetime and longer periods of "quiet beam" for users
  - Reduce vacuum chamber overheating
- BPM R&D
  - Prototyping new DFE and considering AFE upgrade
  - Comparison with "Libera Brilliance"
- Install new IDs to fully built beamlines

Lattice upgrade

  - Limited effort: "split-bend' approach and emittance down to 200 pm-rad
  - Or build a fully diffraction-limited (ε_x & ε_y) in the NSLS-II tunnel!

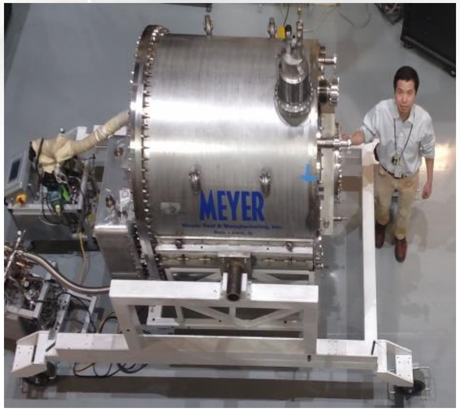

Cryomodule

Harmonic cavity*

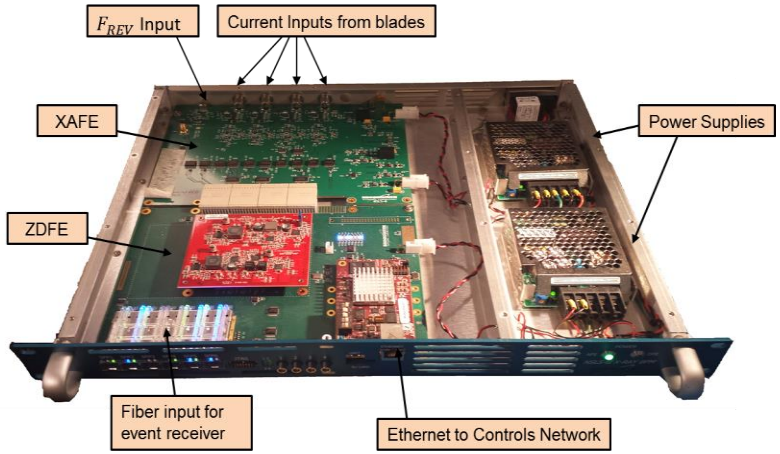

X-Ray BPM Electronics

*Originally built by Niowave under SBIR

Future upgrade

NSLS II: Brightness/Coherence driven science cases

- Brightness/coherence driven experiments
  - Experiments using a coherent X-ray beam or using diffraction limited focusing X-ray optics
  - ***Low emittance → resolution and scan time***
- Hard X-ray Nanoprobe Beamline:
  - cutting-edge multimodality 3D nano-tomographic with 5-10 nm resolution
  - Nano Diffraction from Nanosheet: study next-generation microprocessor, *e.g.* in IBM's new nanosheet technology, down to 7 nm thickness, state-of-the-art (10-14 nm commercial)
- Coherent Hard X-ray Scatting beamline: study real time thin-film growth, ~10 nm length scales and ~ms and μs time scales

FinFET

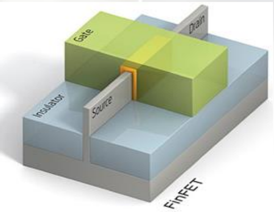

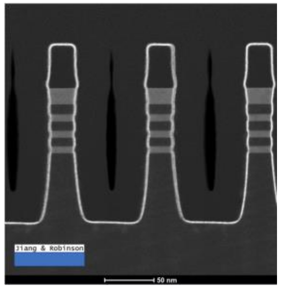

Nano-diffraction (5 sec/frame)

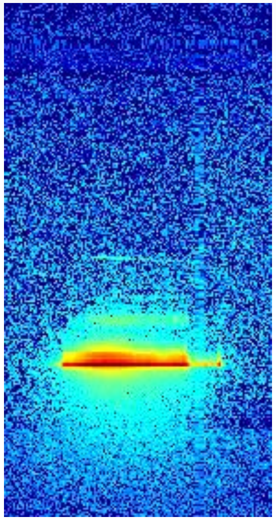

https://en.wikipedia.org/wiki/Semiconductor_device_fabrication

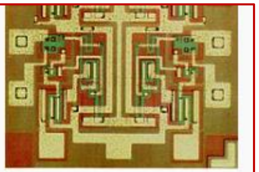

- 130 nm – 2001
- 90 nm – 2003
- 65 nm – 2005
- 45 nm – 2007
- 32 nm – 2009
- 22 nm – 2012
- 14 nm – 2014
- 10 nm – 2016
- 7 nm – 2018
- 5 nm – 2019

3D nano-tomographic

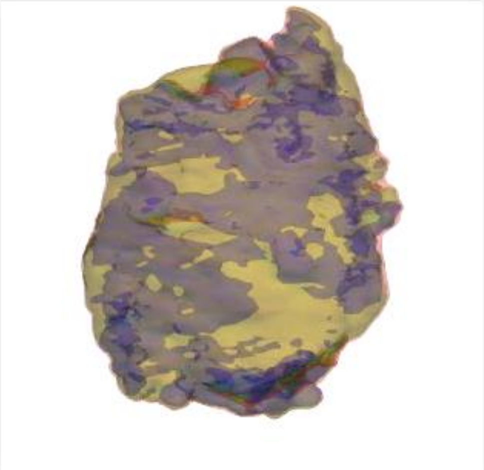

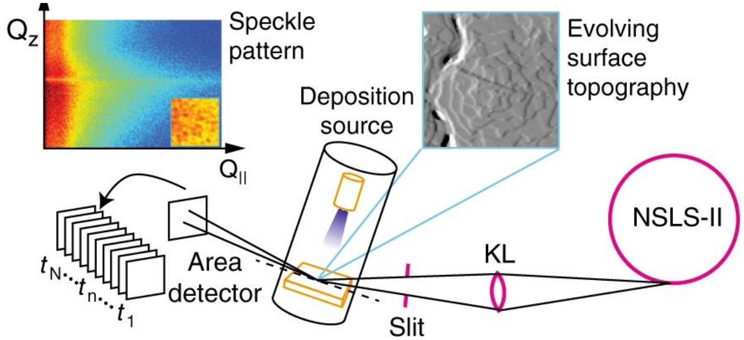

C_{60} film growth on polycrystalline graphene/SiO_2

Headrick et al. Nature Comm. (2019)
https://doi.org/10.1038/s41467-019-10629-8

Synchrotron light source: today and tomorrow

- Two order magnitude of emittance reduction: increasing brightness and coherence
- Transition from Double- and Triple-Bend Achromats to Multi-Bend Achromats
- All MBA-based projects consider significant increase of N_d

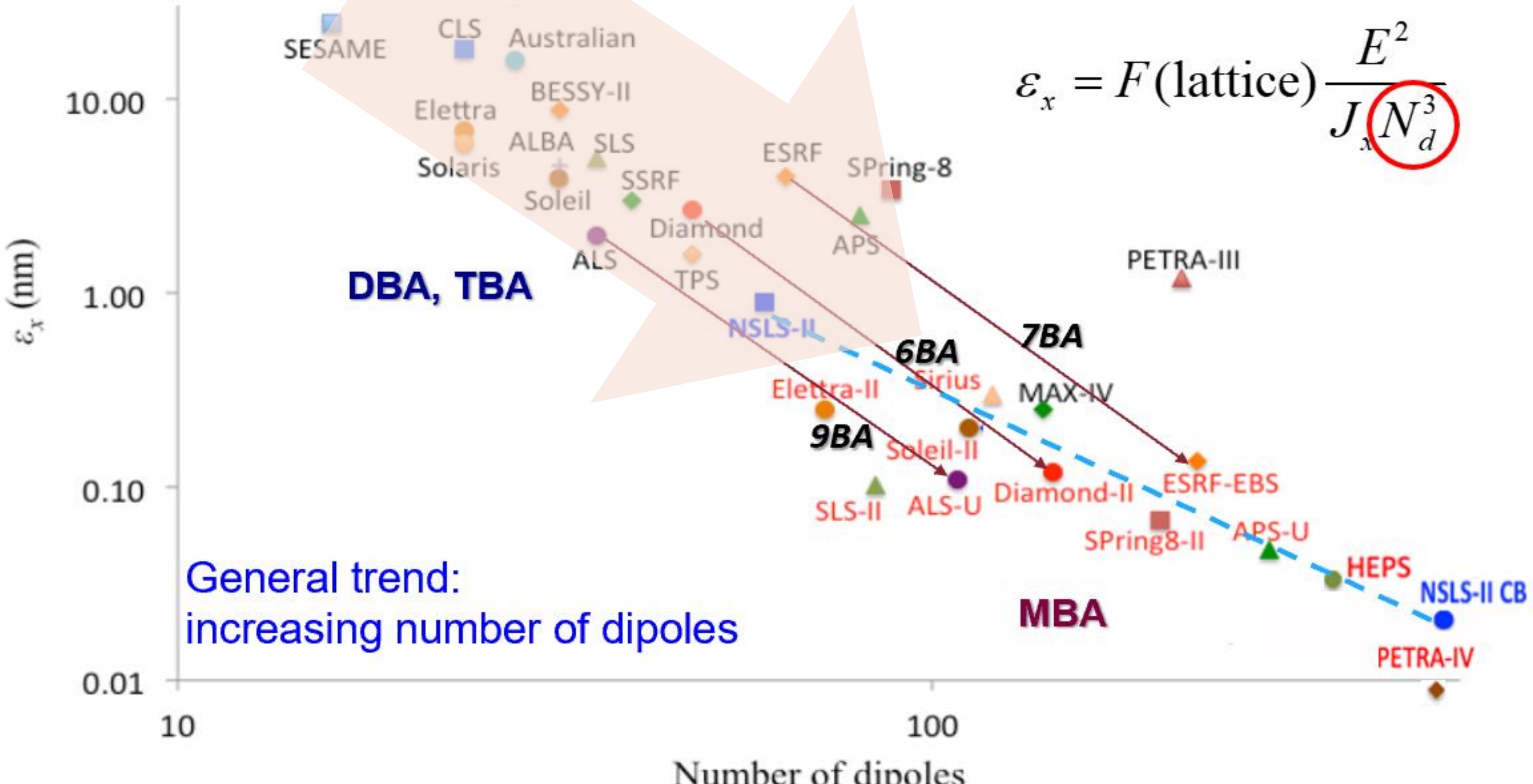

From DBA to MBA

- Trend of minimizing emittance of modern storage rings translates into reduction of η_x and β_x in their lattice dipoles
- Further reduction of emittance leads to dense and complex MBA lattices
- An alternative solution, Complex Bend (CB): preserve substantial room for SR lattice elements

DBA (NSLS II), 900 pm·rad

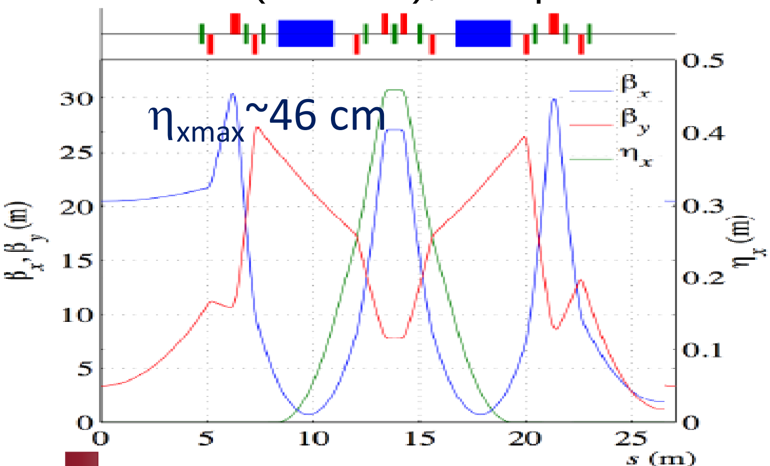

7BA[1] (MAX IV), 250 pm·rad

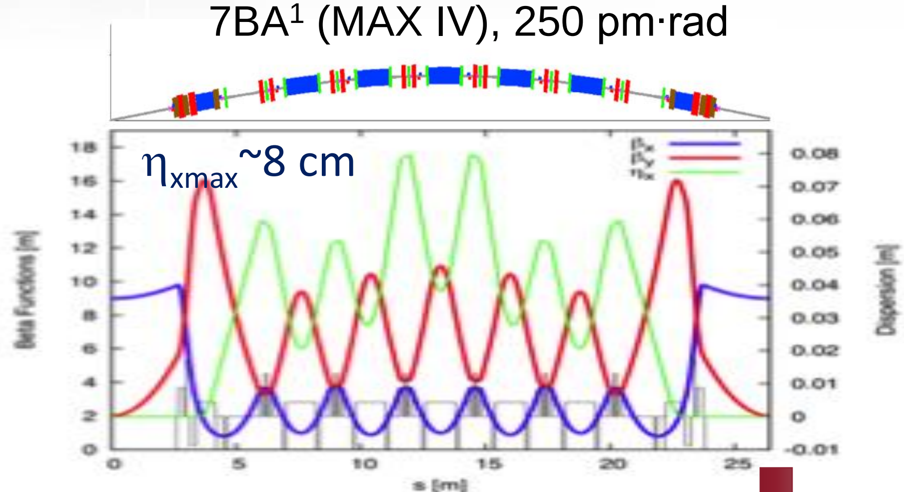

CB (example for NSLS II),19 pm·rad

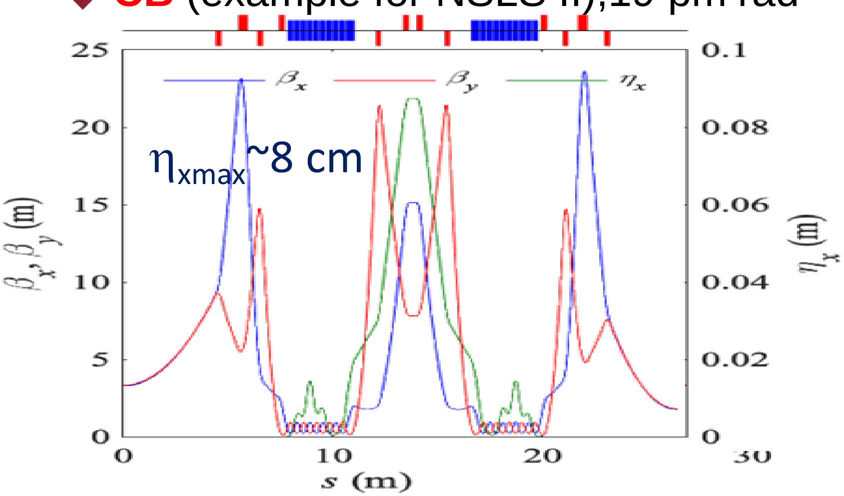

19 BA[2] (MAX IV upgrade),16 pm· rad

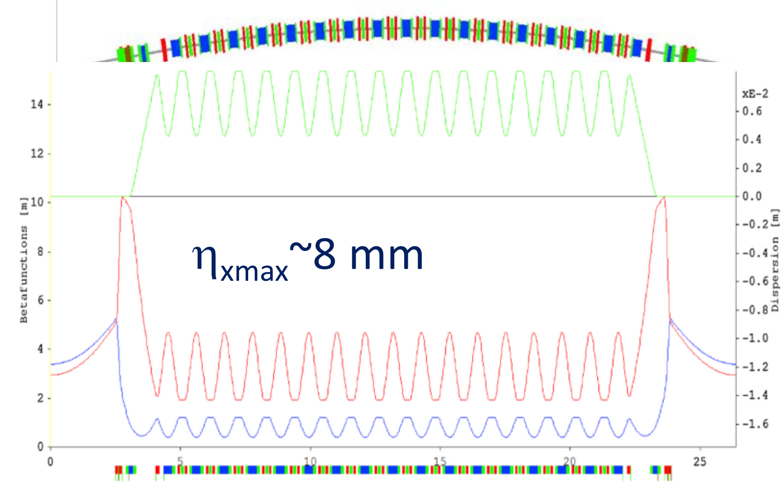

1. P.F.Tavares et al., J. Synchrotron Radiat. 21 (2014) 862-877.
2. P.F.Tavares et al., J. Electron. Spectrosc. Relat. Phenom.224 (2018) 8-16.

Complex bend: Properties of the element

- Properties of the element
- Integration into lattice design
- Magnet design
- Prototype of Complex Bend

$$\varepsilon_x = F \frac{E^2}{J_x N_d^3} \overset{CB}{\Rightarrow} F \frac{E^2}{J_x \left[N_d N_p\right]^3}$$

Transition from individual dipoles to multiple dipole poles

- APS DBA: 40x2=80 dipoles→
- APS-U MBA: 40x7=280 dipoles→
- NSLS-II upgrade: 30x2x10=600 poles

Complex Bend concept

- Complex Bend: a bending element consisting of dipole poles, interleaved with strong focusing and defocusing quadrupole poles, QF-D-B-D-QD-D-B-D (**CB**)
- Conventional long dipole → a sequence of short strong focusing poles
- Produce small beta-function and dispersion, resulting in substantially emittance reduction

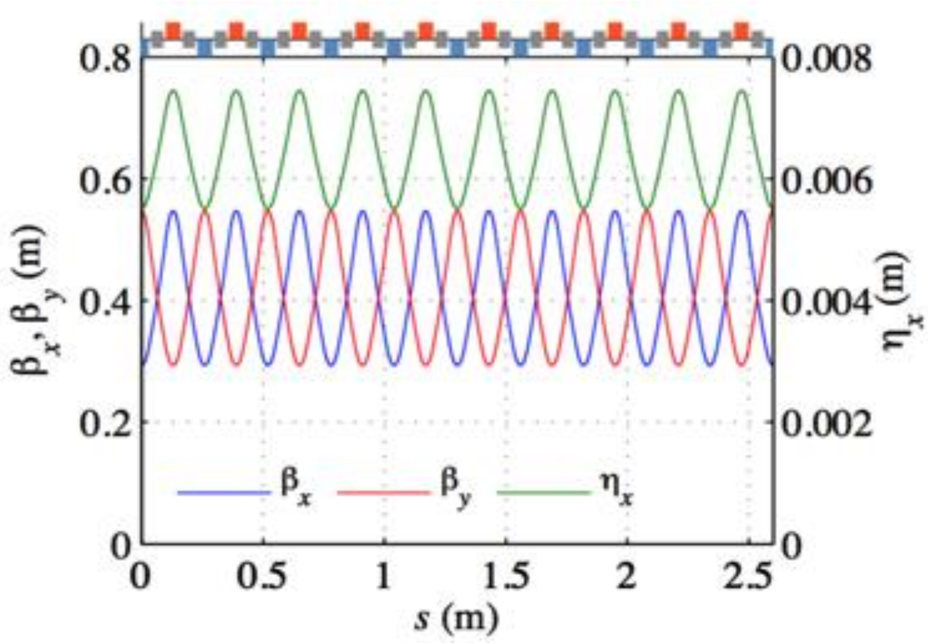

Complex Bend I

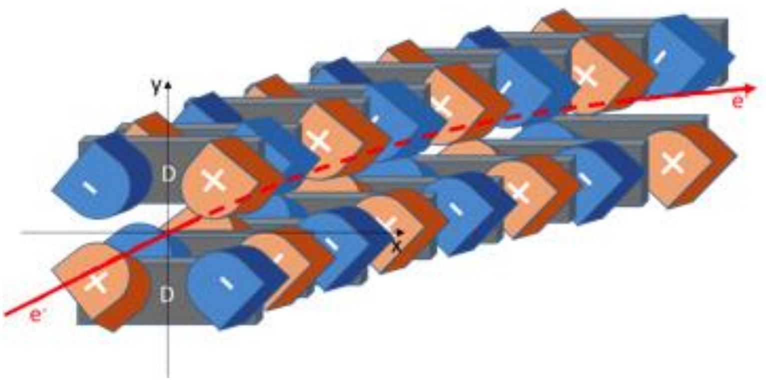

T. Shaftan

G. Wang, , T. Shaftan *et al.*, Complex bend: Strong-focusing magnet for low-emittance synchrotrons, Phys. Rev. Accel. Beams 21, 100703

Analytic results of Complex Bend

Length of 1 cell $L_{CB} = 2(L_Q + L_B + 2L_D)$ $k_{CB} = \dfrac{2\pi}{L_{CB}}$

Beta function $\beta_x(s) \approx \overline{\beta_x} - \Delta\beta_x \cos(k_{CB} s)$

Dispersion $\eta_x(s) \approx \overline{\eta_x} - \Delta\eta \cos(k_{CB} s)$

Analytic expressions of $\overline{\beta_x}$, $\Delta\beta_x$ and $\overline{\eta_x}$, $\Delta\eta_x$ have been derived for $K_{1F} = -K_{1D} = K_1$

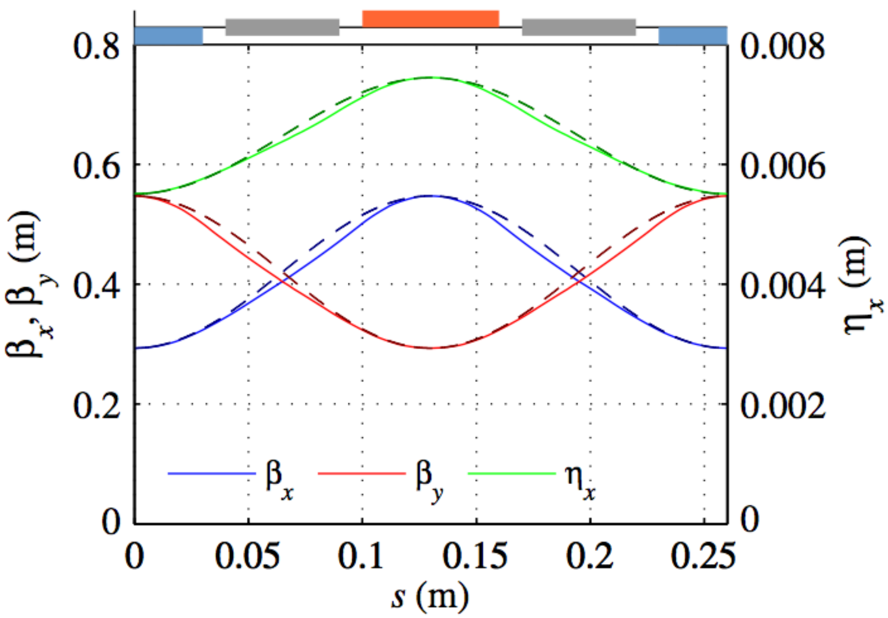

Emittance

$$\varepsilon_x \approx C_q \gamma^2 \frac{\overline{\eta_x}^2}{R_B \overline{\beta_x}}$$

Chromaticity

$$\xi \approx -\frac{N_p}{\pi} K_1 \frac{\Delta\beta}{k_{CB}} \sin\left(\frac{k_{CB} L_Q}{2}\right)$$

Complex bend vs DBA

- A Complex Bend magnet (10 periods): same total bending angle and length as NSLS-II dipole results in **70 pm-rad** emittance, 30 times lower emittance than NSLS-II DBA lattice
- Reach **13 pm-rad** emittance with 4.5 m CB
- Very strong quadrupole magnets (hundreds T/m) → *~1 mm horizontal shift introduce required dipole field*

	NSLS-II dipole	Complex bend I
Length, m	2.6	2.6 (0.26 per cell)
Bending field, T	0.4	1.05
Bending angle, rad	0.105	0.105
K_1, m^{-2}	0	+100 / –80
β_{max} / β_{min}, m	3.7 / 0.7	0.42 / 0.24
η_{max} / η_{min}, mm	137 / 0	4.7 / 3.6
Emittance, nm	**2.09**	**0.07**

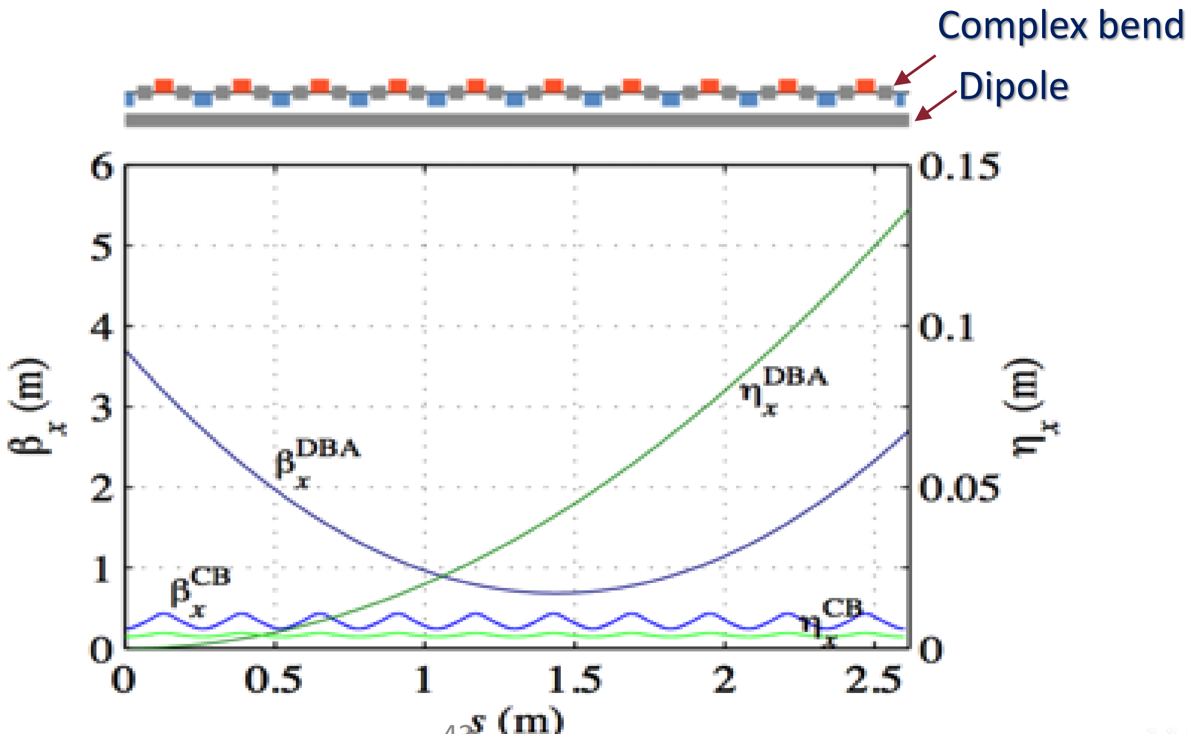

Evolution to CB II and CB III

- CB II&III: offer substantially reduce the device length by removing the dipole poles
- CB II Bending: shift the quadrupole poles offset
- CB III Bending: PMQ installed into a wide gap of the conventional electromagnet

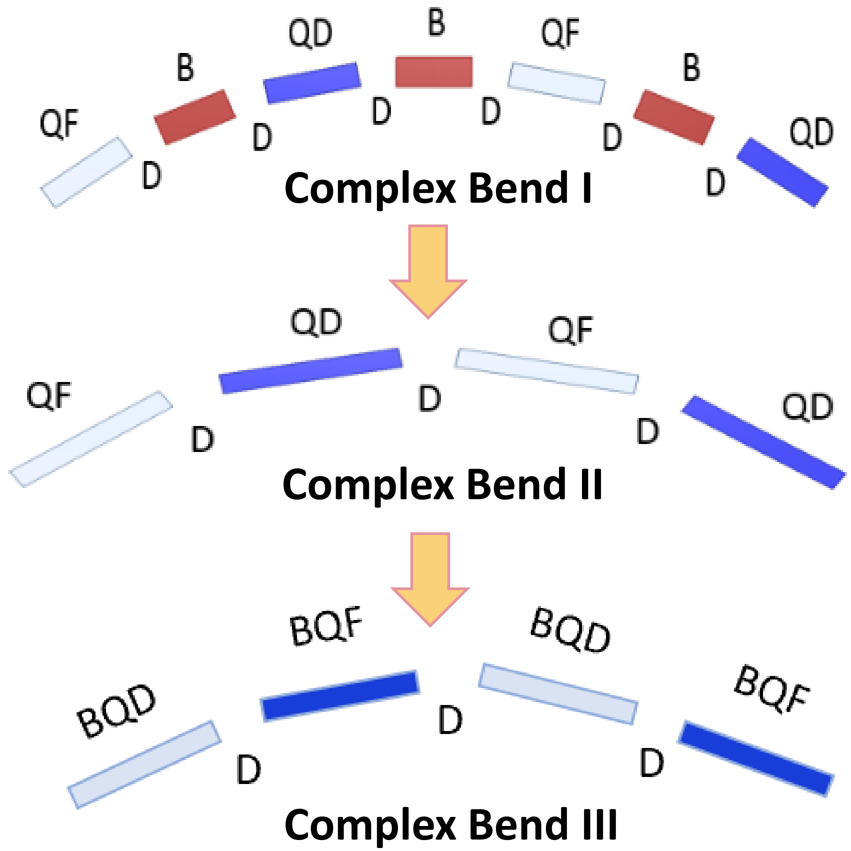

1.5 cells of CBII geometry

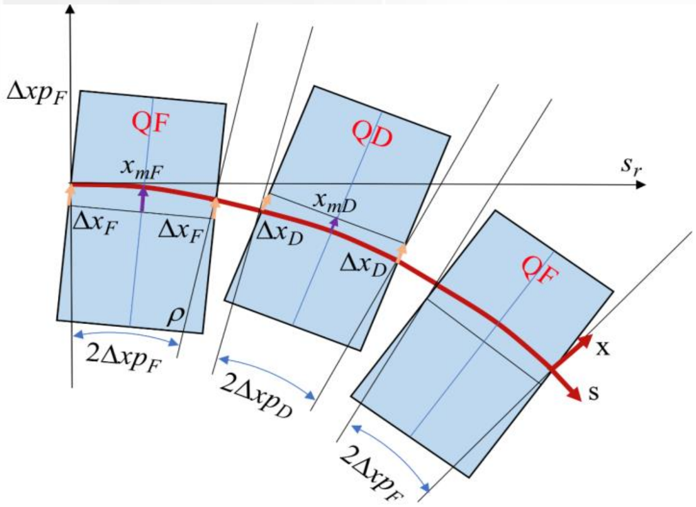

Permanent Quads inside an electromagnet dipole for CBIII

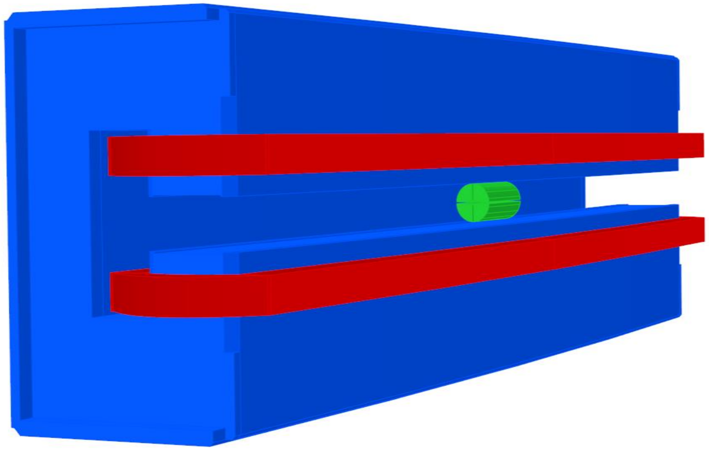

G. Wang, T. Shaftan, V. Smaluk et al., Complex Bend II: A new optics solution , Phys. Rev. Accel. Beams 22, 110703, 2019

Stability constraint of ring beam dynamics

- Quads in dipole: synchrotron integral I_4, dominated from quads K_1 in each pole → specific condition to maintain positive partition numbers $J_{x/z}$
- Ring can be stable if the relationship between the B fields of focusing and defocusing poles is satisfied

$$I_4 = \oint \frac{\eta}{\rho}\left(\frac{1}{\rho^2} + 2K_1\right)ds \qquad I_2 = \oint \frac{ds}{\rho^2}$$

$$J_x = 1 - \frac{I_4}{I_2}, \qquad J_z = 2 + \frac{I_4}{I_2}, \qquad \varepsilon_x = F\frac{E^2}{J_x[N_d N_p]^3}$$

Periodic structure case, $N_F = N_D = N_Q, L_F = L_D = L_Q$

$$I_4 \approx \frac{N_p 2\eta_{Fav} K_{1F} L_Q}{\rho_{Fav}^3} - \frac{N_p 2\eta_{Dav} K_{1D} L_Q}{\rho_{Dav}^3}$$

Theorem: stability condition to maintain positive partition numbers

$$\eta_{Fav} K_{1F}^2 B_{Fav}^3 + \eta_{Dav} K_{1D}^2 B_{Dav}^3 \approx 0$$

G. Wang, T. Shaftan, V. Smaluk et al., Complex Bend II: A new optics solution , Phys. Rev. Accel. Beams 22, 110703, 2019

Complex bend: Integration into lattice design

- Properties of the element
- Integration into lattice design
- Magnet design
- Prototype of Complex Bend

DCBA lattice and TCBA lattice

Double CB Achromat cell structure

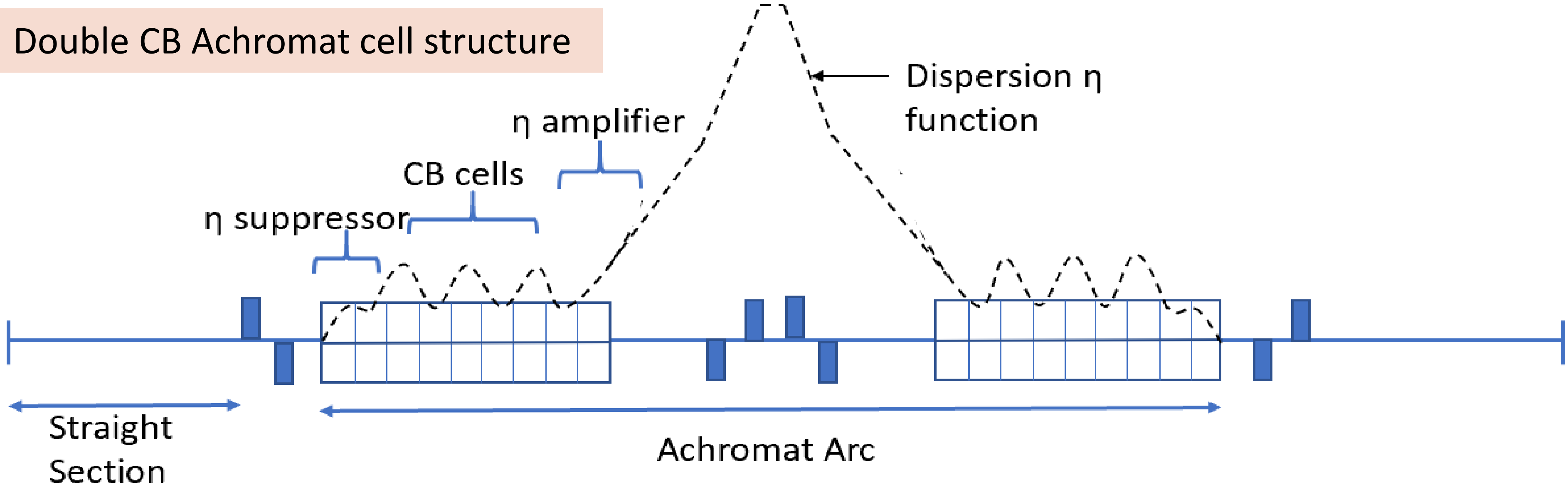

Triple CB Achromat cell structure

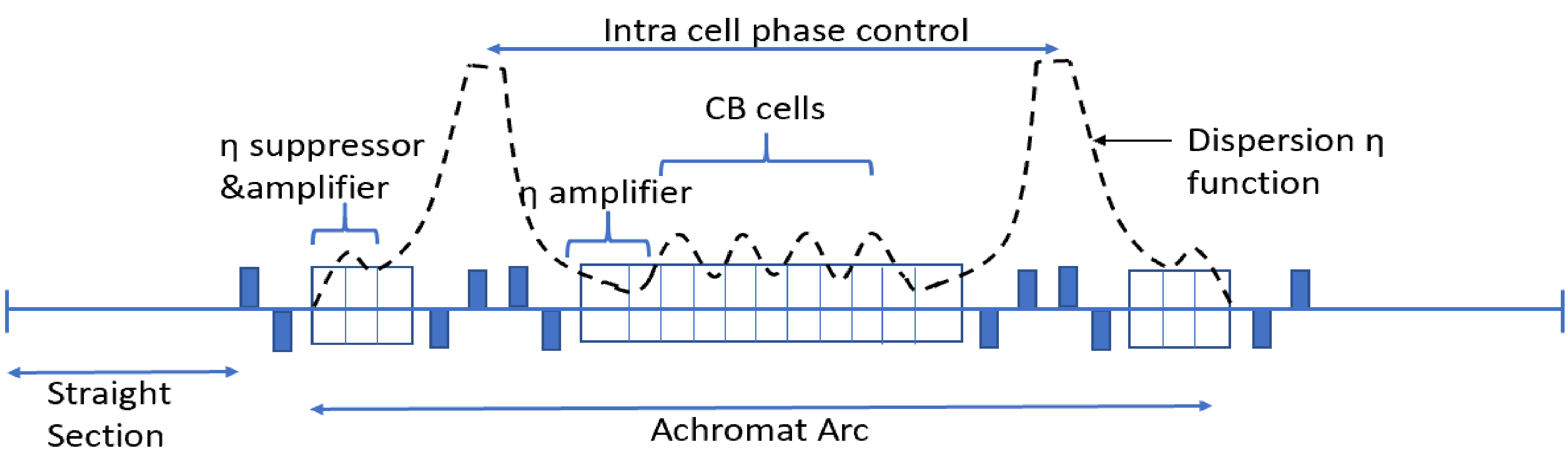

DCBA lattice for NSLS-IIU: 25 pm-rad

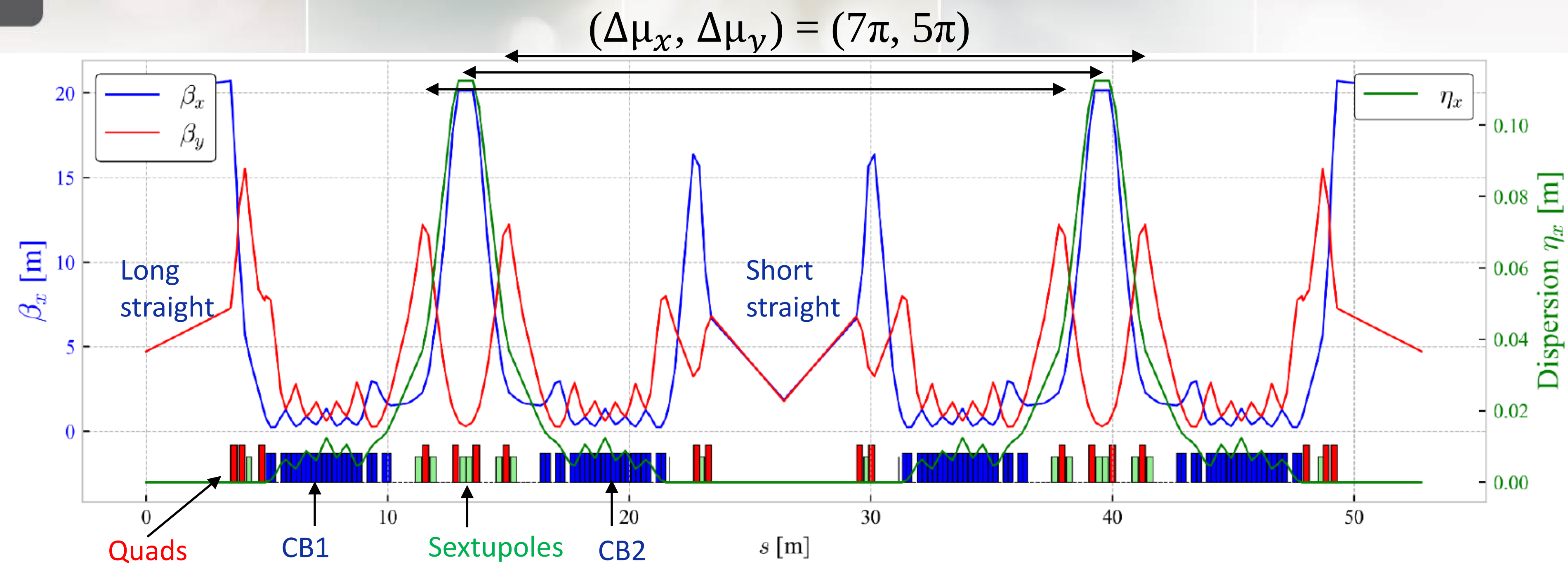

- Similar elements layout as NSLS-II
- Comparable space as DBA lattice for SR other elements
- 2*11 poles CB with gradient ~ 105 T/m
- Phase advance cancellation over one super cell, $\Delta\psi_x = 7\pi$, $\Delta\psi_y = 5\pi$ between sextpoles
- 5 chromatic sextupoles per cell to control chromaticity ($K_2L < 75$ 1/m^2)
- 7 mm*1.5 mm (x/y) dynamic aperture, sufficient for the off-axis anti-septum[1] injection

C. Gough and M. Aiba, TOP-UP INJECTION WITH "ANTI-SEPTUM" , IPAC2017, P774-776

TCBA lattice for NSLS-IIU: 34 pm-rad

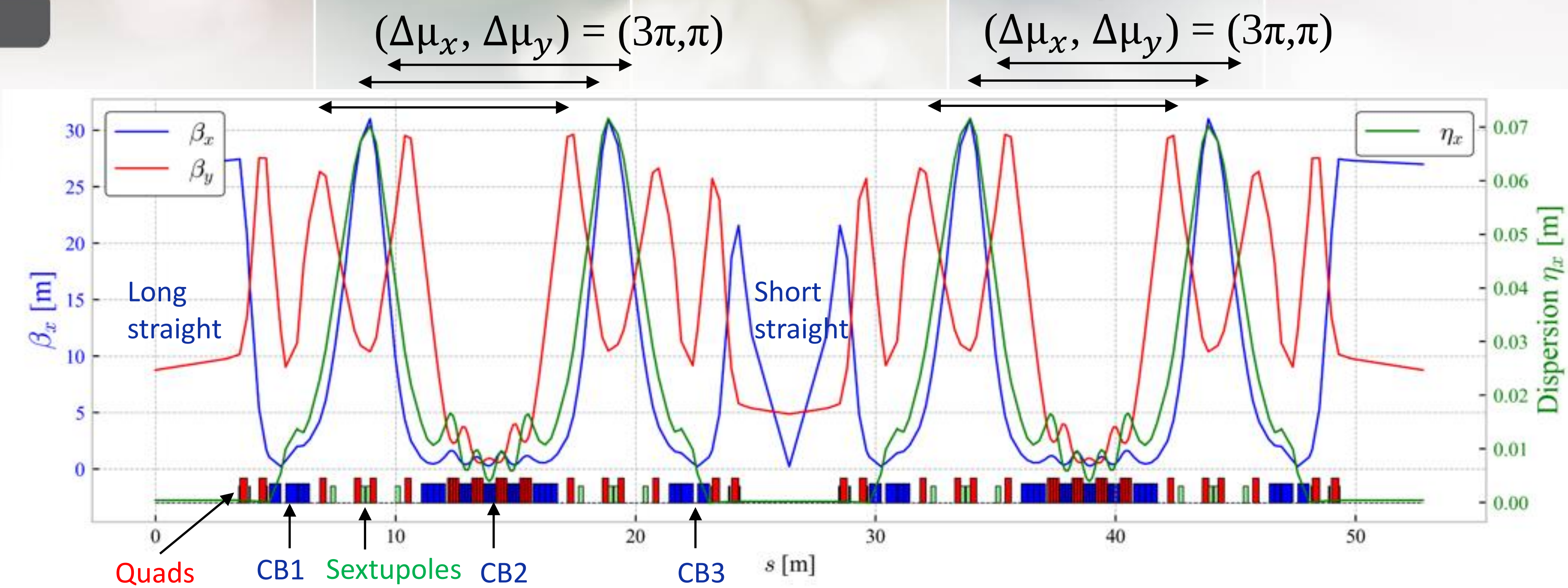

- Three CBs to control dispersion: dispersion bump and dispersion suppression
- Two edge CBs' with lower gradient, thus large physical aperture for ID radiation extraction
- Middle CB (G ~100 T/m) focusing poles with no bending to minimize emittance
- Phase advance within one cell, $\Delta\psi_x = 3\pi$, $\Delta\psi_y = \pi$ between sextupoles
- Two dispersion bumps per cell with 3 families of chromatic sextupoles to control chromaticity ($K_2L < 50$ 1/m^2)
- Long/short straight structure with zero dispersion: insertion devices, RF cavity, injection
- Lattice was optimized (beta, phase, setupole strength) to provide a self-cancellation of geometric Resonant Driving Terms (RDTs) h_{jklm} (j+k+l+m=3) from chromatic sextupoles. Will consider to implement harmonic sextupoles

Y. Hidaka, F. Plassard

TCBA lattice: main parameters

Property	Values
Beam Energy E [GeV]	3
Natural Horizontal Emittance ϵ_x [pm-rad]	34.4
Damping Partitions (J_x, J_y, J_δ)	(1.92, 1.00, 1.08)
Damping Times $(\tau_x, \tau_y, \tau_\delta)$ [ms]	(25.98, 50.01, 46.52)
Ring Tunes (ν_x, ν_y)	(85.180, 22.140)
Natural Chromaticities $(\xi_x^{\text{nat}}, \xi_y^{\text{nat}})$	$(-215.187, -198.267)$
Corrected Chromaticities $(\xi_x^{\text{cor}}, \xi_y^{\text{cor}})$	$(+2.366, +2.625)$
Momentum Compaction α_c	6.25×10^{-5}
Energy Loss per Turn U_0 [keV]	317
Energy Spread σ_δ [%]	0.076
(β_x, β_y) at Long-Straight Center [m]	(19.82, 3.09)
(β_x, β_y) at Short-Straight Center [m]	(0.22, 2.30)
max (β_x, β_y) [m]	(24.98, 32.26)
min (β_x, β_y) [m]	(0.20, 0.53)
η_x (min, max) [mm]	$(-0.1, +71.9)$
Length of Long Straight L_{LS} [m]	7.020
Length of Short Straight L_{SS} [m]	4.220
Circumference C [m]	792.000
Circumference Change $\Delta C/C$ [%]	+0.005
Number of Super-periods	15
Source Point Diff. at LS $(\Delta x, \Delta z)$ [mm]	$(-3.79, +22.89)$
Source Point Diff. at SS $(\Delta x, \Delta z)$ [mm]	$(+15.34, +15.05)$
Revolution Frequency f_{rev} [kHz]	378.526

TCBA lattice: higher order correction

- The lattice performance is strongly limited by higher order effects from the sextupoles, especially amplitude dependent tune shift (ADTS) terms
- **Octupoles are used here to correct large linear ADTS**
- The strength of 3 octupole families are calculated from solving the linear system to cancel for the horizontal, vertical and cross term of linear amplitude detuning
- Oct[H, V, C] are placed in the lattice with large $\frac{\beta_x}{\beta_y}$, large $\frac{\beta_y}{\beta_x}$, and $\frac{\beta_x}{\beta_y} \approx 1$
- Octupoles are placed in dispersion region close to the chromatic sextupoles

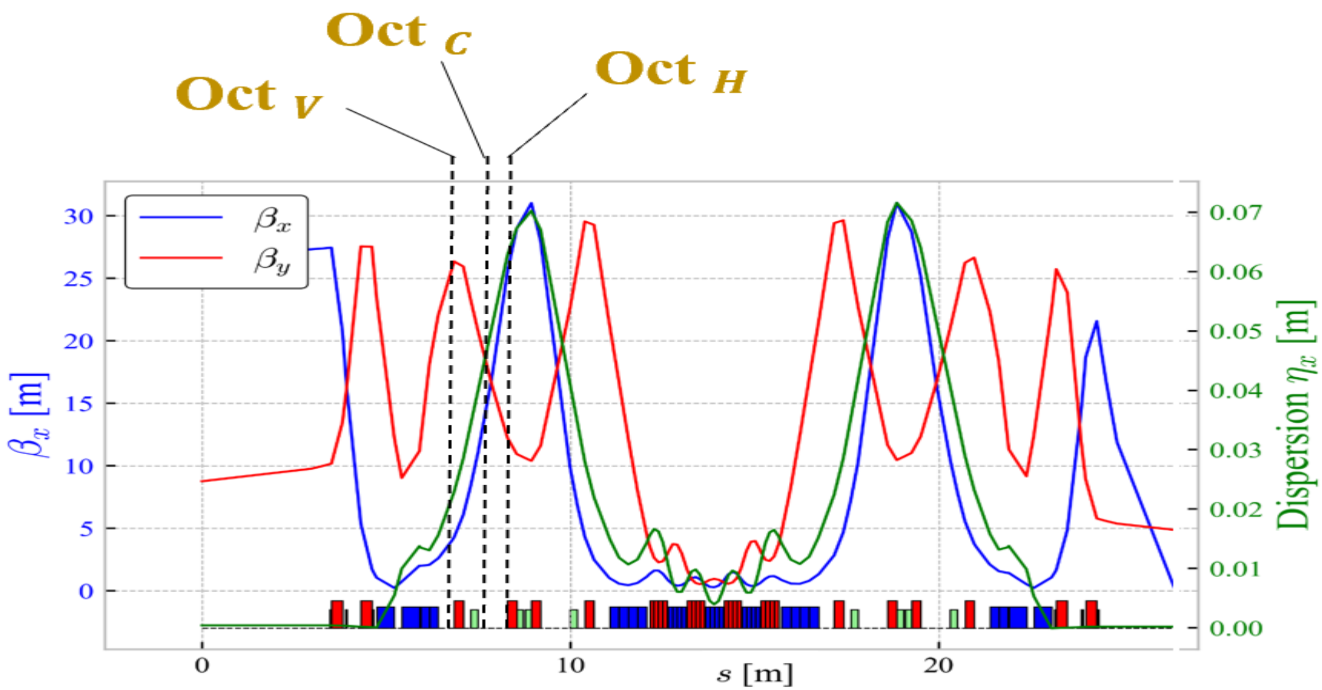

F. Plassard

TCBA lattice: property with and w/o Octupoles correction

- 3 families of octupoles: K_3L ~ 3600 $1/m^3$
- Improve ADTS
- Improve on-momentum DA: ±~3mm → ±~9mm
- Reduce momentum acceptance due to increase of 2nd order chromaticity. Need further optimization

Without Octupoles

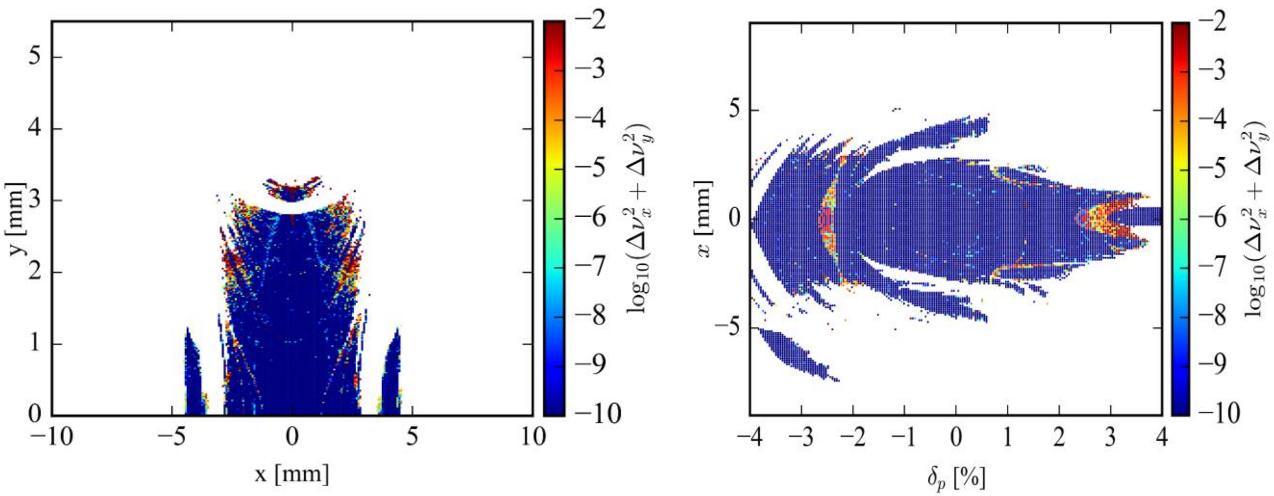

With Octupoles

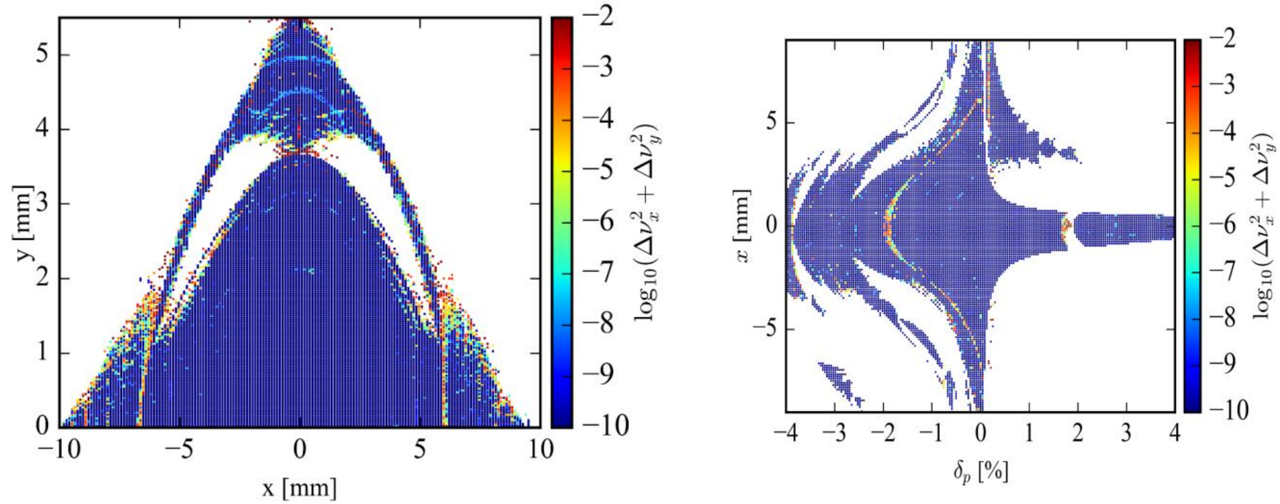

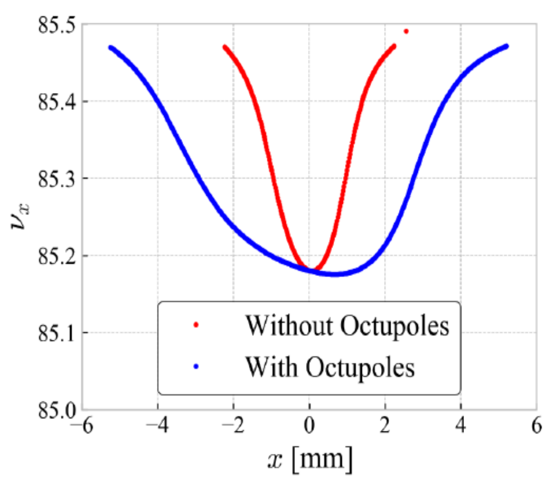

F. Plassard

TCBA lattice: error sensitivity

- The on-momentum DA can be mostly recovered after correction
- Among the different seed simulated, the emittance stays within **~5%** for the TCBA after a full optimization

Errors	*Value*
Transverse misalignment $\sigma_{\Delta x,y}$	**20 µm**
Roll angle σ_{roll}	**200 µrad**
Quad strength error Δk/k	$\mathbf{5\times 10^{-4}}$
Sextupole/ Octupole strength error Δk/k	$\mathbf{1\times 10^{-3}}$

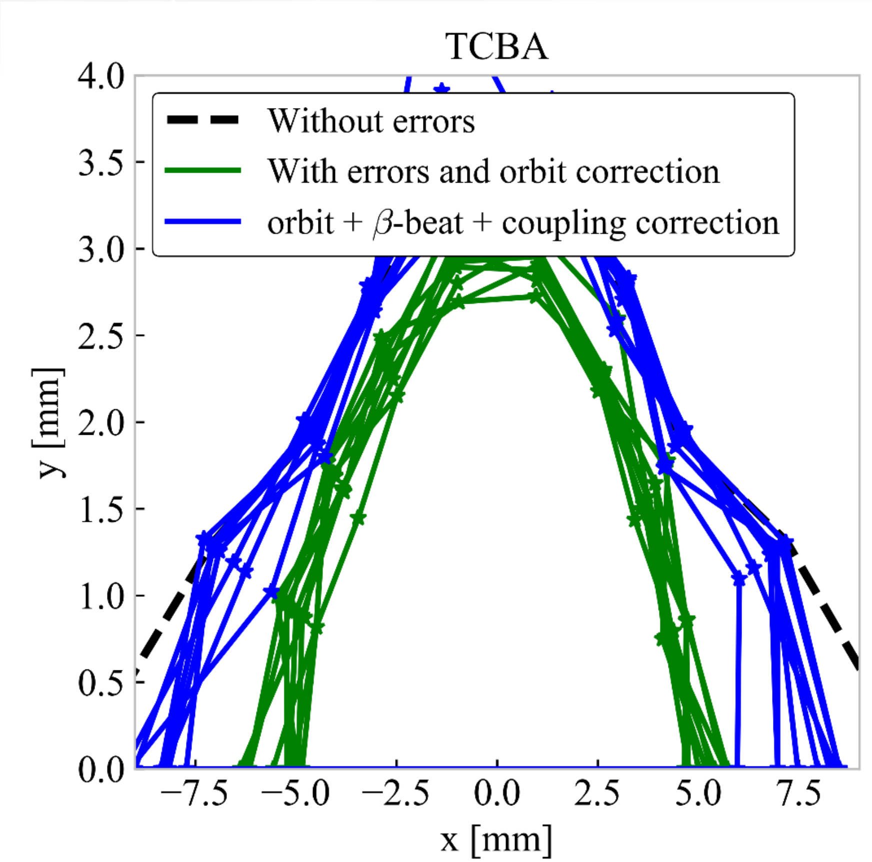

Complex bend: Magnet design

- Properties of the element
- Integration into lattice design
- Magnet design
- Prototype of Complex Bend

Conceptual Design of a High Gradient CBIII Quadrupole

- Require Quads offset by 1~2 mm for a dipole field, resulting in large harmonic field of B_3 to B_6
- Superimposed Dipole and Quadrupole fields
- External H-shaped electromagnetic dipole with 90 mm aperture
- Halbach PMQ assembled inside a round 90-mm aluminum vacuum chamber
- Ante-chamber for the extraction of x-rays and for pumping via NEG strips.

External H-shaped electromagnet dipole for Complex Bend III

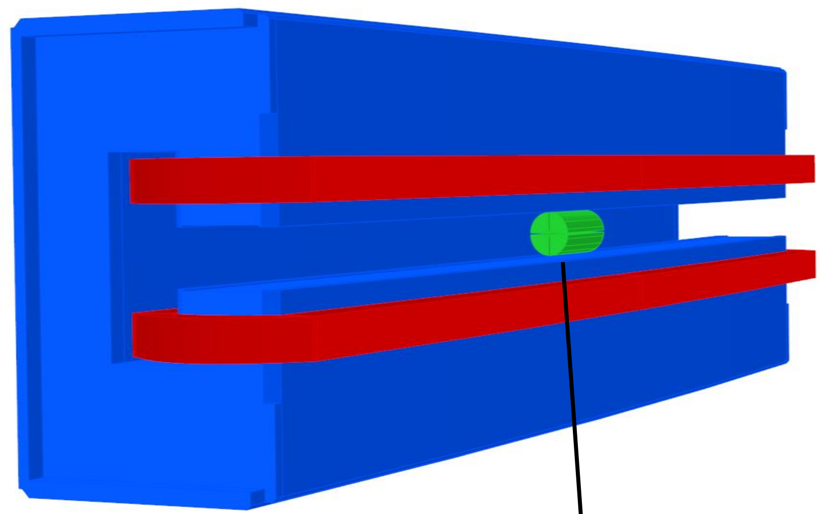

Out-of-Vacuum PMQ

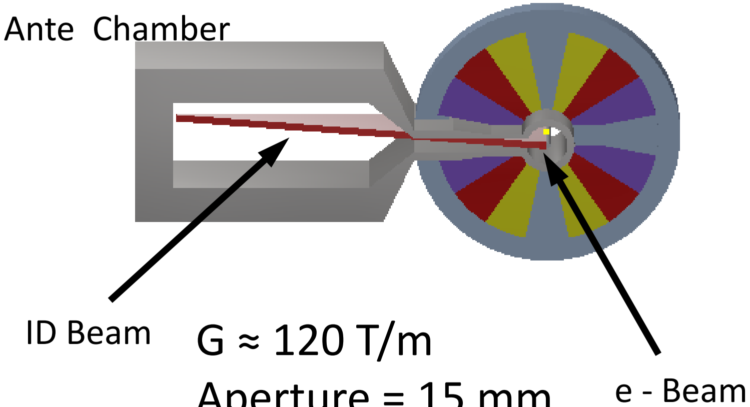

G ≈ 120 T/m
Aperture = 15 mm

In-vacuum PMQ

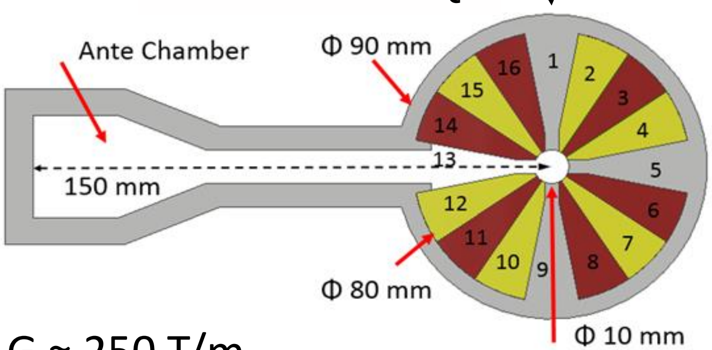

G ≈ 250 T/m
Aperture = 10 mm

S. Sharma et al. "High gradient quadrpoles for low emittance synchrotrons," IPAC2019, Melbourne, Australia, May 2019.

S. Sharma

Halbach PMQ for Complex Bend

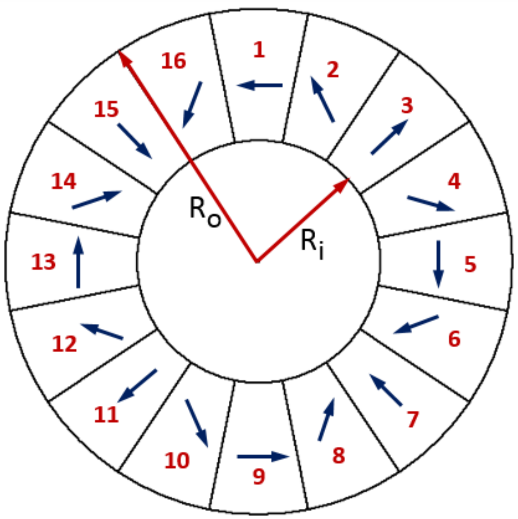

Standard 16-wedge Halbach PMQ
G~358 T/m

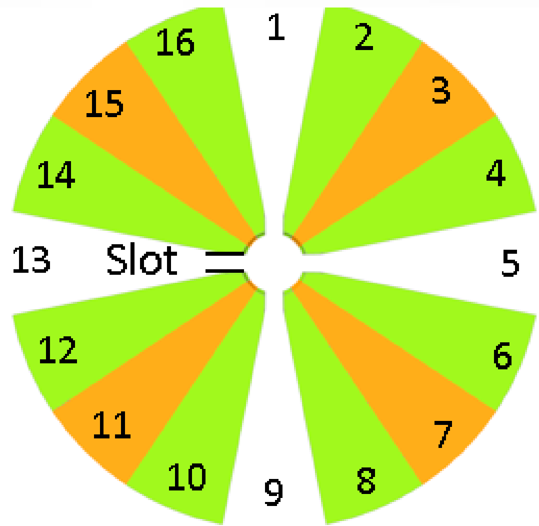

Modified PMQ with exit slot for the x-ray beams.

- G: 254 - 215 T/m with variable slot height
- 3D Opera model, NdFeB with low remanent field, 1.12 T

PMQ field harmonics at 2 mm radii with 3 mm Slot

n	An	Bn
1	-0.1	0.1
2	-0.2	10^4
3	-0.3	0.1
4	0.0	0.2
5	0.0	0.0
6	0.0	-55.0*
7	0.0	0.0
8	0.0	0.0

*can be reduced by shimming of the poles

Complex bend: Prototype of Complex Bend

- Properties of the element
- Integration into lattice design
- Magnet design
- Prototype of Complex Bend

Prototype of Complex Bend

- Engineering design for a prototype of CB
- Downscaled *E* from 3 GeV to 50-200 MeV
- Maintain high gradient magnetic field and reduce the size of the pole and overall length of CB
- Build the prototype from an array of Permanent Magnet Quadrupoles (Commercially available)
- Commission the device at NSLS-II Linac dump line in FY21
- Characterize properties of the CB element, create kick maps and study both geometric and chromatic aberrations
- Motivate the future proposal to build the full-scale CB for 3 GeV machine.

Parameters of CB and NSLS-II dipole

	Complex Bend	50-200 MeV prototype
Length, m	3.1	0.62
Bending field, T	0.26/0.49	0.026/0.049
Cell length, cm	62	12.3
Bending angle per cell, °	1.2	1.2
Gradient, T/m	250/-250	150/-150

Summary and outlook

- Achieved 400 mA top off routine operation and demonstrate beam current 500 mA
- Achieved designed beam emittance, ε_x= 0.9 nm-rad and ε_y = 8 pm-rad
- Beam orbit motion stabilized <10% beam size
- Provided 5000 hrs operations with 97% reliability for 28 beamlines
- 3rd RF cavity will be installed and commissioned in FY21
- Harmonic cavities are needed for 500 mA diffraction limit emittance operation
- *Consider an option path for NSLS-II upgrade*
- Proposed a new concept of a lattice element “Complex Bend” = a sequence of dipole poles interleaved with strong alternate focusing so as to maintain the beta function and dispersion oscillating at low values
- Comprising the ring lattice with Complex Bends, instead of regular dipoles, we already went to 25 and 19 pm-rad emittance while localizing bending to a smaller fraction of the storage ring circumference
- Explored different lattices with DCBA and TCBA structure and achieved >5 mm DA
- Conceptual designs for high-gradient quadrupoles with Halbach permanent-magnet quadrupole, ~250 T/m
- Developed an engineering design, 150 T/m, for a prototype of CBIII and will be tested at Linac dump line with 50-200 MeV beam

Acknowledgements

- Accelerator division director: T. Shaftan
- Accelerator Coordination: G.M. Wang, J. Choi, Y. Hidaka, R. Smith, B. Wahl
- Accelerator Physics: V. Smalyuk, G. Bassi, X. Yang, Y. Li, L.H. Yu
- Beam Operations group: E. Zitvogel, R. Fliller, T. Summers, M. Santana, G. Weiner, E. Zeitler, R. Rayner, C. Gardner, P. Marino…
- RF group: J. Rose, F. Gao, J. Cuppolo, J. Culpin, B. Holub, C. Marques…
- ID group: T. Tanabe, J. Rank…
- Vacuum group: C. Hetzel…
- Diagnostics and Instrumentation group: D. Padrazo, B. Bacha, B. Kosciuk, J. Mead
- Electrical Engineering: G. Ganetis, S. Buda, A. Castablanco, D. Oldham, W. Louie
- Controls: Y. Tian, K. Schroff, Y. Hu, K. Ha
- Mechanical Engineering group: L. Doom, S. Sharma, M. Loftus, A. Hussein, C. Spataro, F. Karl…

Many thanks to the Complex Bend design team for upgrade:

- Bassi, Gabriele; Blednykh, Alexei; Choi, Jinhyuk; Fliller, Raymond; Hidaka, Yoshiteru; Hidas, Dean; Kosciuk, Bernard; Plassard, Fabien; Shaftan, Timur; Sharma, Sushil; Smalyuk, Victor; Spataro, Charles; Tanabe, Toshiya; Tchoubar, Oleg; Wang, Guimei;